ISOLATION OF PRIMARY CANINE SATELLITE CELLS

David A. Detwiler

A dissertation submitted to the faculty of the University of North Carolina at Chapel Hill in partial fulfillment of the requirements for the degree of Doctor of Philosophy in the Department of Pathology and Laboratory Medicine.

Chapel Hill
2012

Approved by:
Joe N. Kornegay D.V.M – Ph. D.

Nancy L. Allbritton M.D. – Ph.D.

Nobuyo Maeda – Ph.D.

Xiao Xiao – Ph.D.

Joan Taylor – Ph.D.

Martin K. Childers D.O. – Ph.D.

John Olsen – Ph.D.

Abstract

DAVID A. DETWILER: Isolation of Primary Canine Satellite Cells
(Under the direction of Joe N. Kornegay D.V.M. – Ph.D.
and Nancy L. Allbritton M.D. – Ph.D.)

Duchenne muscular dystrophy (DMD) is a debilitating disease that principally affects striated muscles (skeletal and cardiac) and is the most severe form of muscular dystrophy. Disruption of the dystrophin gene is the primary cause of disease leading to excessive muscle damage. Regenerative processes counterbalance damage but individuals with DMD eventually succumb to immobilizing loss of strength and death from cardiac and pulmonary complications in their late teens and twenties. Golden retriever muscular dystrophy (GRMD) is a large animal model with better mimicry of the human disease than mouse models. Its development and characterization are critical to developing therapies for DMD. The cells primarily responsible for the regenerative response in skeletal muscle are satellite cells. These cells have been characterized at the protein level previously with only minor differences found between normal and dystrophic cultures. However, satellite cells have not been characterized at the transcriptional level. Pax7, MyoD, Myogenin and Utrophin act as critical members in the path to myogenesis. In this work, we have looked at the mRNA variation in cells collected from normal and GRMD animals and found substantial differences in mRNA expression profiles. These finding are also reflected in cell fusion experiments done on the same cultures. Studying these proteins and mRNAs in vitro under growth and differentiating conditions can help

characterize satellite cells in the GRMD model. To sort through the heterogeneity of satellite cell populations, clonal cultures are needed to better characterize protein and mRNA patterns in these cells. Methods such as limiting dilution or flow cytometry require considerable time and resources to clone and verify large numbers of colonies for analysis. Micropallet array technology is a cell sorting method that permits clonal culture of large numbers of cells in very small spaces. Employing its flexible nature, micropallet array technology has been adapted to culture primary satellite cells from the GRMD model. Using these adaptations, clonal colonies have been cultured and shown to proliferate on tri-partite micropallet arrays. This forms two sister colonies where one sister colony can be analyzed and the other reserved for continued culture and downstream experiments.

Acknowledgements

University of North Carolina – Chapel Hill School of Medicine
Department of Pathology and Laboratory Medicine
Joe N. Kornegay D.V.M – Ph. D.
Nancy L. Allbritton M.D. – Ph.D.
Janet Bogan B.S. - CMAR
Dan Bogan B.A.
Nobuyo Maeda Ph.D.
Xiao Xiao Ph.D.
Joan Taylor Ph.D.
Martin K. Childers D.O. – Ph.D.
John Olsen Ph.D.
Nickolas Dobes B.S.
Pavak Shah B.S.E
Heather Doherty Ph.D.
Mathew Medlin Ph.D.
NIH
MDA
National Center for Canine Models of DMD (NCDMD)

Table of Contents

List of Tables

List of Figures

List of Abbreviations

4-VP:	4-vinyl pyridine
AA in PS:	Acrylic Acid in Polystyrene
AAV:	Adeno-associated Virus
BMD:	Becker's Muscular Dystrophy
DAPI:	4′,6-Diamidino-2-phenylindole dihydrochloride
DGC:	Dystrophin Glycoprotein Complex
DMD:	Duchenne Muscular Dystrophy
DMEM:	Dulbecco's Modified Eagle's Media
DNA:	Deoxyribonucleic Acid
DSHB:	Developmental Studies Hybridoma Bank
ECM:	Extracellular Matrix
EDTA:	Ethylenediaminetetraacetic Acid
ESEM:	Environmental Scanning Electron Microscope
FACS:	Flow Cytometry Assisted Cell Sorting
FBS:	Fetal Bovine Serum
GRMD:	Golden Retriever Muscular Dystrophy
GSHP:	German Short Haired Pointer
MDX:	Muscular Dystrophy X-Linked
MHC:	Myosin Heavy Chain
mRNA:	messenger Ribonucleic Acid

MSC:	Mesenchymal Stem Cell
NCAM:	Neural Cell Adhesion Molecule
ND:YAG:	Neodymium-Doped Yttrium Aluminum Garnet
PAA:	Polyacrylic Acid
PBS:	Phosphate Buffered Saline
PCSCs:	Primary Canine Satellite Cells
PDMS:	Polydimethyl Siloxane
PEB:	Post Exposure Bake
PFA:	Paraformaldehyde
PP#:	Preplate number (1 through 6)
PS:	Polystyrene
RNA:	Ribonucleic Acid
RT-PCR:	Real Time Polymerase Chain Reaction
RTA:	Relative Telomerase Activity
TC:	Tissue Culture
THF:	Tetrahydrofuran
UV:	Ultraviolet

List of Symbols

µg	Microgram
µm	Micrometer
µL	Microliter
mm	Millimeter
g	Gravity (Normal) or Gram
β	Beta

Chapter 1

Introduction

Background and Significance

Muscular dystrophy is a spectrum of diseases that affects principally striated (skeletal and cardiac) muscles [1-5]. The most severe form of muscular dystrophy, Duchenne Muscular Dystrophy (DMD), presents a progressive loss of strength in the skeletal muscles and leads to muscle atrophy. Complications from progressive muscle deterioration limit the lifespan of affected individuals to two to three decades. Several animal models for DMD have been developed, with the two most important being the mouse (MDX – Muscular Dystrophy X-Linked) and the canine (GRMD - Golden Retriever Muscular Dystrophy). The mouse model has been used extensively to examine the underlying disease physiology [6, 7]. The canine model, GRMD, better mimics the human disease in severity and is a size relevant model [8, 9]. Currently there are no clinically available therapies that correct or halt the progression of the disease, though clinical trials are underway [10-12].

Genetics and Occurrence

Duchenne Muscular Dystrophy is a genetic disease primarily related to the functions of the dystrophin gene and affects the skeletal muscles [10-12]. The gene is encoded on the X-chromosome, Xp21, and subsequently primarily occurs in males [1, 13]. DMD affects one in 3500 to 7500 males [14]. Many cases of DMD are inherited. However, due to the large size of the dystrophin gene, 2.4 megabases in length, spontaneous mutations are a common occurrence [13, 15, 16]. These can be small point mutations or deletions that can create a stop codon or change the reading frame to large

deletions. Either way, a truncated, poorly functioning or non-existent dystrophin protein results.

Dystrophin Function

Dystrophin is found in many tissue types outside of skeletal muscle including neural, smooth muscle and cardiac tissues, though transcriptional variants may be found in these tissues [17]. Its primary role is that of mediating force transduction from the actin-myosin network in the skeletal muscle to the laminin and collagen extracellular matrix surrounding the muscle fibers that come together to form tendons [18]. However, dystrophin does not do this alone. It is a major part of the dystrophin glycoprotein complex (DGC) [18]. Without dystrophin this complex does not form and forces are unevenly transmitted through the cell membrane of the muscle cells, the sarcolemma, causing tears in the membrane. Tears allow extracellular calcium to enter the cells causing the fiber to undergo necrosis [19, 20]. Utrophin is the autosomal homologue of dystrophin and is up-regulated in DMD. Though genetically homologous, it can't fully replace the functions of dystrophin and organize the formation of the DGC [21, 22].

Clinical Diagnosis and Disease Progression

DMD is diagnosed in early childhood due to a lagging in physical development and a loss of strength. Without any viable clinical therapies, boys have a progressive loss in strength and are often confined to a wheelchair early in their second decade of life. The weakened state of the muscles is due to a lack of capacity to deal with forces coming into and generated by the muscles. This damages the muscle fibers and leads to a regenerative cycle to rebuild the muscle. This cycle of damage and repair continues for years leading to identifiable histological pathologies, including most notably individual

and grouped muscle fiber necrosis. There are increases in the amount of fibrous connective tissue and fat within the body of the muscle [23, 24]. Muscle fibers are variably sized, ranging from small ones undergoing regeneration to others that are markedly enlarged due to hypertrophy. DMD patients suffer from cardiac and breathing problems as their heart and diaphragm begin to fail, causing many patients die in their late teens to twenties.

Animal Models

DMD has been identified in numerous vertebrates. However, only a few models of DMD have been characterized in mice, cats, and dogs [8, 9]. Many studies have been completed in mdx mice, because of the ease of keeping a colony, the short breeding time, and the ability to do many replicates. Much of our molecular understanding of DMD has come from the study of the mdx mouse [6, 7]. The mdx mouse remains relatively normal clinically, but in contrast, dystrophin-deficient dogs develop progressive disease similar to the human condition [8, 9]. The most commonly studied canine model is golden retriever muscular dystrophy (GRMD). GRMD is characterized by a point mutation between the sixth and seventh exon of the dystrophin mRNA that causes the seventh exon to be excluded from the nascent mRNA [25]. This leads to a reading frame shift and the formation of an early stop codon, resulting in a truncated non-functional protein. However, some cells can create alternate combinations of the exons and translate truncated but functional protein, resulting in relatively normal muscle fibers, termed revertant fibers [1, 26]. Another canine model, the German short haired pointer (GSHP), has a large genetic deletion, essentially amounting to a dystrophin knock-out [27]. These

GSHP dogs do not have revertant fibers, thus facilitating studies to define the immune response with forms of genetic therapy that restore dystrophin.

Therapies

There are no viable therapies for DMD that exist as a standard of care, although research has led to clinical trials on several fronts. Therapies fall into three basic categories with hybrid combinations. The first therapeutic approach is pharmaceutical. A long used drug in the form of the corticosteroid, prednisone, can reduce some of the symptoms of DMD, thus, for instance, delaying the time at which affected boys must transition to wheelchairs [28, 29]. Other drugs target stop codon read-through and exon skipping to get around point mutations that cause an early termination of the protein [30]. Some of these drugs are in clinical trials.

Another major means of therapy is to manipulate the genetics of the individual. This can be achieved through systemic delivery of DNA or RNA based vectors that are capable of introducing a gene or RNA transcript that can replace the dysfunctional dystrophin gene or modify the mRNA that the nucleus produces. These methods have met with some substantial success in restoring dystrophin production and reestablishing the DGC at the sarcolemma [22]. Viruses can also be used to introduce a modified gene or RNA. Two common categories of viruses that are used to introduce a gene are adeno-associated viruses (AAV) and retroviruses. Regardless of the vector, the gene that is delivered is restricted in size by the packaging capacity of the virus [31, 32]. Viral therapy has had some success in integrating recombinant genes into dystrophic mice and dogs [10, 32, 33].

Cell based therapies have been developed for two main reasons. The first is due to the success of bone marrow transplantation in curing a number of diseases. This has served as the paradigm for cell transplantation. The second is that cell transplantation could potentially restore some or all of the muscle mass associated with muscle atrophy as the individual ages. There are two potential sources for cells. Allogeneic cells can be collected from donors, immunologically matched and transplanted into the recipient. Allogeneic cells provide the opportunity to restore native dystrophin to the muscles with all of the molecular regulation in place, assuming a normal donor. Alternatively, autologous transplantation involves the collection of a stem cell population from the patients and then modifying the cells to replace or restructure the dysfunctional dystrophin.

Several types of cells have been used in DMD studies. The first type is myoblasts and their stem cell, the satellite cell. Satellite cells occupy an anatomical niche between the sarcolemma of the myofiber and the basement membrane. This position is what allowed satellite cells to be first identified in 1961 by Katz and Mauro. Satellite cells remain quiescent when there is no need for muscle repair and then activate quickly to provide numerous myoblasts to repair damage. Furthermore, they are able to self-renew to maintain the number of satellite cells [34].

Myoblast transfer therapy was shown, by Partridge et al, to be a viable in-vivo, cell-based therapy [35]. Studies using the mdx mouse showed that myoblasts could be successfully delivered to muscles and that they could then fuse with the host myofibers and contribute proteins [36, 37]. This led to human clinical trials in the 1990's [38]. Though allogeneic transplantation has been shown to be successful in mice, similar

transplants in dogs and humans have met with limited success due to failure to produce functional gains in strength or mitigate disease progression [39, 40]. Immune rejection and limited cell survival may have restricted the success of these studies [3, 39]. Satellite cells remain of great interest as they are the natural stem cell involved with muscle regeneration and are readily available from simple biopsies.

Besides the satellite cells and associated myoblasts, there are many adult stem cell populations throughout the body capable of multi-lineage differentiation [41-44]. Bone marrow has two sets of cells that have been tested for contribution to muscle regeneration. Both are readily obtainable during the entire lifetime of a DMD patient or GRMD dog. The first are bone marrow stromal cells (MSCs). These mesodermal cells line bone trabeculae. Stromal cells injected directly into the muscle, without a forced differentiation toward myogenic lineage, contribute very little to muscle regeneration in mouse models [45, 46]. The second set of bone marrow cells contributing to muscle regeneration are the hematopoietic stem cells. Dell'Agnola et al used the GRMD model, termed CXMD in their studies, to determine the contribution of an allogeneic bone marrow transplant to regenerating muscle [47]. Despite successful allogeneic engraftment, bone marrow-derived cells did not contribute either skeletal muscle or muscle precursor cells.

More recently, vascular associated stem cells, called mesoangioblasts, have been used to contribute to muscle regeneration [48-52]. These cells are multipotent, with capacity to give rise to osteogenic, adipogenic, myogenic, and endothelial lineages. The initial work was done in embryos of chick, quail, and mouse and was then taken to the canine model [51, 52]. This study showed that clinically-relevant cell mass can be

obtained for transplant into GRMD dogs. A variety of surface markers, including c-met, M-cadherin, VE-cadherin, P-selectin, and VEGF-receptor 2 but not CD34, CD45 or CD31, have been identified on these cells [52]. Mesoangioblasts can be injected directly into the muscle or intra-arterially. Polyclonal populations of cells were injected in the femoral artery so as to allow cells direct access to the downstream capillary beds [52]. Outcomes varied from normal disease progression to an almost normal histological phenotype. However, questions have been raised about the outcome parameters used and the role that immunosuppression may have played in improvement [53].

Characterization of cell types

With the use of cellular therapies, there is a need to understand the exact nature of the cells being used. Transplanted bone marrow will repopulate an irradiated animal. Characterization of the cell populations within the biopsy is critical to limit potential side effects, treat the disease with a greater degree of precision, and better understand the fundamental biology of the stem cell. The same is true for cell populations used in myogenic therapy. Cell size, shape, proliferation rate and protein expression are all important in the characterization of a particular population. Satellite cells and myoblasts have been characterized from mouse, human and dog [34, 54-57]. These studies have focused on the protein expression of cells, either intracellular where immunohistochemistry is used or vital cell techniques, such as flow cytometry, where cells can be characterized and subsequently used in downstream experiments. Antibody resources for mouse models and humans have been well developed but resources for dogs lack the same level of diversity and availability.

The myogenic potential of cells has also been characterized in vitro [55, 57]. This involves differentiating the cells down the myogenic pathway towards the production of multinucleated myotubes in cell fusion experiments. Quantitation of the number of cell fusions and the number of nuclei per myotube are used to demonstrate the ability of cells to contribute to muscle regeneration in vivo. Though useful in demonstrating the ability of cells to differentiate, it is not a measure of the success that a cell will have after being transplanted into the body. A number of differences have been characterized in cells derived from different species, mostly in regard to surface antigens used in flow cytometry.

Micropallet arrays

Micropallet arrays are a new tool that can be used to sort adherent cells [58-60]. They are fabricated using a photolithography technique and a light sensitive polymerization reaction of a photoresist [58]. A mask permits UV light to pass through and cause a photoinitiator to crosslink monomers into a solid form, **Figure 1.1A**. Unpolymerized material is dissolved away revealing the pattern of individual structures, termed micropallets. This array is then treated with a chemical that creates a hydrophobic layer. When aqueous solutions such as culture media are applied, virtual air

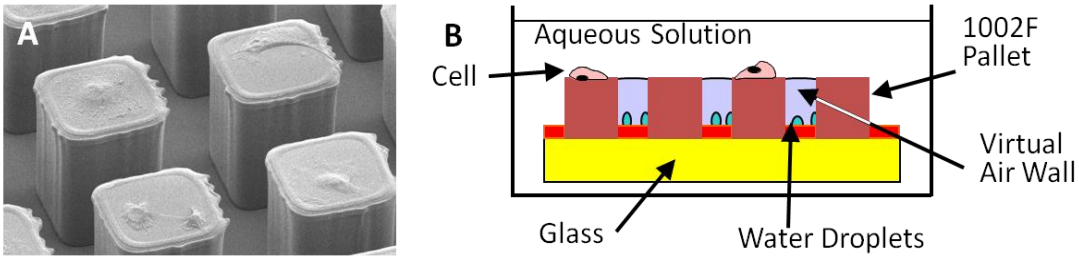

Figure 1.1. Micropallet arrays. A) Scanning Electron Microscopy of micropallet array with HeLa cells. Array dimensions are 50 × 50 µm (L × W). B) Schematic of a side view of a functional micropallet array.

walls are created between the micropallets. This permits cells seeded onto the array to only interact with the top surface of the micropallets **Figure 1.1B**. Individual micropallets, which contain cells, can then be released from the surface with the aid of a focused laser pulse and collected for further culture or analysis [61].

Micropallet arrays provide a means to clonally culture and isolate cells based on a wide range of characteristics [58, 62, 63]. These include the presence or absence of fluorescently tagged proteins and additional criteria not available to flow cytometry including their adherent morphology, growth rate, and other dynamic behavior [58, 60]. With the large number of pallets available on an array, the cloning and isolation of moderate to large numbers of cells is greatly simplified over standard tissue culture cloning techniques. Micropallet arrays have previously been used to clone and sort tumor cells, murine embryonic stem cells, and other cell lines [58, 60, 62]. While cell lines have been adapted to cell culture conditions for numerous generations, more physiologically relevant primary cells are not so adept at adhesion to artificial surfaces. A tailored culture environment is required to meet the needs of these primary cells.

The 1002F photoresist from which the micropallet arrays are fabricated has been shown to be suitable for culturing tumor cell lines [58, 60, 62, 63]. In some instances the 1002F required an additional coating such as collagen or fibronectin for cell attachment and growth. An alternative means of applying a protein or other material to the surface of an array is contact printing [64]. This process involves spreading a thin layer of dissolved protein or other material on a standard glass slide. The micropallet array is then inverted and briefly pressed into contact with the coated slide. The array is removed from the slide and now contains a thin layer of material on the surface of the

micropallets. Cells can then be cultured on this alternative surface. This means the micropallet technology can be adapted and optimized to a variety of cell types including stem cells.

Chapter 2

Isolation, Culture, and Characterization of Primary Canine Satellite Cells from the GRMD Model

Introduction

Duchenne Muscular Dystrophy (DMD) is an inherited, progressive neuromuscular disease caused by mutations in the dystrophin gene and is characterized by ongoing cycles of degeneration and regeneration leading to progressive loss of muscle strength. No treatment has been shown to halt progression of the disease, although gene, cell, and pharmacologic approaches have been studied. Cell based therapies, whereby normal or genetically-corrected autologous cells are expanded in culture and transplanted into dystrophic individuals, in principle, offer the advantage of actually restoring muscle mass. Satellite cells, myoblasts, and other myogenic stem cells are the most promising candidates for transplantation.

Despite promising results in the dystrophin-deficient mdx mouse, myoblast transplantation was largely ineffective in DMD patients due to the combined deleterious effects of early cell death, immune rejection, and poor migration beyond the transplant site [2, 5, 39]. The use of earlier muscle progenitor cells circumvents these issues to some extent, in that stem cells have a greater capacity to replicate, are less prone to immune rejection, and can potentially "home" to muscle [4, 52, 65-67].

Over the past 25 years, extensive studies have been undertaken in golden retrievers with muscular dystrophy (GRMD), a model with a spontaneously occurring splice site mutation in the dystrophin gene [68]. This model has increasingly been used as a preclinical model for various therapeutic approaches, including cell-based therapy.

Despite the successes of cell transplantation in mice, the GRMD based experiments fall in line with the human trials as both were unable to achieve a therapeutic implantation of myoblasts (Kornegay JN, unpublished observations) [39, 40]. Because of the negative human findings, clinical trials were halted in the late 1990's.

Satellite cells occupy an anatomical niche between the sarcolemma of the myofiber and the basement membrane. This position is what allowed satellite cells to be first identified in 1961 by Katz and Mauro [69]. The satellite cells must be able to remain quiescent when there is no need for muscle repair and then activate quickly to provide numerous myoblasts needed to repair damage. Furthermore, they must be able to self-renew to maintain the satellite cell population [34].

The source of satellite cells for most muscles during development is the somites [70-72]. After myogenic induction in the somite, Pax3 and MyoD regulate the embryonic myoblast populations during migration and proliferation. Once muscles have been formed, myoblasts transition to a population of quiescent satellite cells. Work with Pax3- or c-Met-null mice has shown a failure of muscle development, save for a few myoblasts in the limbs [50]. These lone myoblasts are positive for CD34 and Flk1, markers associated with hematopoietic and endothelial cells. Pax7-null mice have no adult satellite cells, and mononuclear cells isolated from muscle do not undergo myogenesis in culture [73, 74].

The satellite cells and myoblasts are known to express several transcription factors which determine, maintain and differentiate the myogenic lineage. In the adult animal, Pax7 is the primary regulator [74, 75]. Expression of Pax7 protein maintains cells in an undifferentiated state and inhibits the expression of genes (MyoD, Myf5,

Myogenin and Mrf4) that regulate the differentiation process. These myogenic regulatory factors are up-regulated in sequence during the proliferative phase after satellite cell activation [54, 66, 76, 77]. They promote expansion of the satellite cells and myoblasts but also encourage terminal differentiation. Once myogenin protein is expressed in myoblasts, there is a cascade towards terminal differentiation and formation of multinucleated myotubes. At this point, terminal differentiation proteins, such as utrophin, are strongly expressed to help the cells execute functions of muscle fibers [78, 79]. Studying the progression of this cascade of expression provides insight regarding genes that drive myogenic differentiation in dogs and allows characterization of these cells in culture.

Satellite cells and myoblasts can be readily obtained through small muscle biopsies. Any isolation technique requires the muscle fibers to be separated to expose the satellite cells. This requires the use of enzymes, typically collagenase and trypsin [80, 81]. Digested material is then passed through sieves to remove muscle fibers and collect mononuclear cells in the remaining fluid. From here there are two basic approaches to the isolation of satellite cells, preplate isolation and flow assisted cell sorting (FACS).

The preplate technique is based on the adhesion of cells to polystyrene tissue culture dishes and involves repeated decanting and culture of the supernatant [80, 81]. Satellite cells are generally quiescent, becoming activated only after a stimulus signals the need to repair damage. Thus, in the initial culture plating, these cells are non-adherent and remain in the decanted supernatant. Other undesired cell types, such as fibroblasts and macrophages, are persistently active, performing functions within the muscle. These activated cells adhere rapidly to polystyrene and remain on the surface during the initial

platings when the media is decanted [65, 81]. This preplating technique ultimately results in a satellite-cell-enriched, but nonetheless heterogeneous, mixture of cells.

FACS is a technique that depends on the use of fluorescently labeled antibodies to surface markers, dyes, and light scattering properties to identify and characterize specific properties of cells [82, 83]. To sort viable cells, a repertoire of antibodies must be available for surface markers on the cell. This antibody repertoire exists for mice but is generally lacking for canine models. NCAM1 (CD56) has been used to sort myoblasts isolated from canine muscle in the past [84, 85]. This protein is expressed on activated satellite cells through multinucleated myotubes [78]. Syndecan4 has also been characterized on canine satellite cells [86]. Little else has been done to characterize the GRMD satellite cells with antibodies.

Primary muscle cell cultures have been characterized for mice, humans and dogs. In these studies, isolated cells were analyzed for differential properties under growth and differentiation conditions [83, 87-92]. There has been little difference in the expression of surface markers and internal proteins between dystrophic and normal myoblasts. A few differences in proliferation and differentiation have been found between normal and dystrophic cells from human and mouse but not canine myoblasts [87-89, 91, 92]. Recent reports have characterized several muscle specific proteins, including desmin, myosin heavy chain, and MyoD, in primary cultures from normal and GRMD cells and found no significant differences between the two groups [57, 86]. The mRNA gene expression profile of dystrophic and normal satellite cells and myoblasts has not been studied. Here, we present an mRNA and immunohistochemistry based analysis of

myogenic cells from normal and GRMD dogs during growth and differentiation to analyze their myogenic potential in cell based therapies.

Materials and Methods

Isolation of satellite cells and myoblasts

Cell cultures were established from biopsies taken sterilely at surgery from the vastus lateralis muscle of the pelvic limb from 2 to 4 month old normal (n =6) and GRMD (n =6) dogs (**Table 2.1).** Muscle samples were placed in a bath of PBS containing penicillin, streptomycin and amphotericin B, on ice. Samples were brought into a sterile tissue culture hood for breakdown. Using a razorblade and forceps, fibrous connective tissue was removed. Tissue was minced to a fine consistency, less than 1mm, to allow pieces to fit though the end of a pipette and then digested with collagenase in growth media for one hour. Every 15 minutes, the tissue was triturated through the narrow opening of a pipette. After one hour, the digested tissue was spun down at 800 g for 2.5 min. The supernatant was removed and the pellet was rinsed with PBS and re-spun; pelleting and rinsing was done twice. The myofibers were then treated with 0.25% trypsin solution for 30 min, with trituration every 15 min, to digest the laminin layer and release the satellite cells. The digested material was then passed through 100 and 40 µm screens to remove fiber debris and isolate the cells. Cells were rinsed twice with PBS and put through the

Dog	Desmin	Pax7
Woody	97.6	93.2
Buzz	99	94.9
Pinkman	94.4	72.6
Tuco	92.2	86.4
Jessie	99.6	80.7
Pedro	100	93.1
Hazel	92.4	85.3
Lyle	93.3	85.2
Toto	97.9	92.5
Zeke	95.3	87.4
Lenard	88.2	80.9
Sophie	91.1	82.8

Table 2.1. Normal (blue) and GRMD (red) study groups. Desmin and Pax7 staining percentages from preplates 5 and 6.

preplate procedure. Cells were plated on tissue culture plastic for one hour to remove rapidly adherent cells. Unattached cells were transferred to a 0.1% gelatin coated plate for 24 hrs (preplate 1), and then on to a new plate every 24 hours for up to 5 plates (preplates 2-6). Cells were cultured in growth media consisting of high glucose DMEM (Sigma) with 20% FBS and 100units/mL penicillin and 100ug/mL streptomycin.

Flow Cytometry

Cell cultures were established and passed once. Cells were removed from the culture surface using 0.5% trypsin with 0.25% EDTA for two minutes. Cells were sequentially centrifuged at 1000 g and washed twice with PBS; re-suspended in FACS Fix buffer, 1% formaldehyde, placed on ice for 10 min, spun down and resuspended in FACS Buffer, stained with antibodies to NCAM-1 (5.1H11 from DSHB, Iowa City, Iowa) and allowed to sit on ice for 30 minutes, washed twice with FACS Buffer, stained with anti-mouse-APC secondary, anti-canine CD45-FITC (AbD Serotec, Oxford, UK) and anti-canine CD34-PE (BD Pharmingen, Franklin Lakes, NJ) and allowed to bind antibodies for 30 minutes; washed twice with FACS Buffer and resuspended in 1mL of FACS Buffer; and run through a Cyan flow cytometer (Dako, Carpinteria, CA).

Cell Differentiation

Cells were plated on gelatin coated 96 well plates, for 1 hr with 0.1% gelatin in sterile water for immunohistochemistry (IHC) experiments or T25 flasks (Corning, Corning, NY) for mRNA collection at a density of 10,000 cells/cm^2. Cells were allowed to adhere for 24 hours in growth media, 20% FBS in DMEM. Growth media was then replaced with 2% horse serum in DMEM differentiation media. Medias also contained 100 units per mL penicillin-streptomycin. Cells were fixed for IHC or 200,000 cells were collected

for mRNA at Day 0, Day 3, Day 5, and Day 7. Cells (~ 200,000) for telomerase expression were collected from Day 0, spun down, decanted and snap frozen in liquid nitrogen and stored at -80^{o}C.

Cell fusion studies were conducted to quantify the ability of cultures to form multinucleated myotubes when presented with a differentiation stimulus, low serum media. Cells were plated at 10,000 cells per cm^2 in T25 flasks. Cells were plated in growth media and switched to low serum media at 48 hrs. Hoechst dye was used to label nuclei and fluorescent images were overlaid with brightfield images to count nuclei (**Figure 2.6 A, B, & C)**. Nuclei involved in cell fusions were quantitated and expressed as a percentage of total nuclei involved in cell fusions. Cultures were imaged at Days 1, 3, 5, and 7 with brightfield and DAPI filter. Cells were temporarily stained with Hoechst 33342, 1 µg per mL, to identify nuclei. The total number of nuclei and nuclei associated with multinucleated myotubes were quantitated with the aid of ImageJ (NIH) software. Images were taken with an Olympus IX81 microscope with a Hamamatsu Orca R2 digital camera system with a 10X lens.

Sample Collection and Processing

Cells collected for IHC were fixed for 10 minutes in 4% PFA, permeabilized with 0.5% Triton-X-100 in 1x PBS for 10 minutes, blocked with 2% FBS in PBS for 1 hour and stained with antibodies at 4^{o}C for four hours and then rinsed with three rounds of 2% horse serum in PBS for 5 minutes. Primary antibodies include: Pax7 (DSHB, Iowa City, IO), MyoD (Dako, Carpenteria, CA), Myogenin (DSHB, Iowa City, IO), Myosin Heavy Chain (DSHB, Iowa City, IO), Desmin (Sigma, St. Louis, MO). Secondary antibody (Invitrogen, Carlsbad, CA) was applied at 1:500 for one hour at 4^{o}C. Cells were rinsed

Gene	Forward Primer	Reverse Primer	Taqman Probe
Pax7	AGT ACG GCC AGA CTG CTG TT	AAT GCT CCC CGA GCT TCA TA	Fam AC CTG GCC AAA AAC GTG AGC CTC TCTamra
MyoD	GAA CAC TAC AGC GGC GAC TC	TGT AGT CCA TCA TGC CGT CG	Fam AC GCG TCC AGC CCG CGC TCC AA Tamra
Myogenin	TCC CAC AGT GCC TCC TGC A	TCG GTG GCG AGC AAG TGG T	Fam CC GAG TGG GGC AGC ACC CTG GA Tamra
Utrophin	CTG ACA GCA GCT CTA CCA CA	CCT CCA AGC GTC TGA CAG TA	Fam TG TGG AGG ACG AGC ATG CCC TCA TC Tamra
b-actin	TCG AGA CTT TCA ACA CCC CA	TCC ATC ACG ATG CCA GTG GT	Fam AC GTG GCC ATC CAG GCT GTG CTG Tamra

Table 2.2: Primer and probe sequences for relative gene expression quantitation.

with three rounds of 2% horse serum in 1x PBS for 5 min and incubated with PBS containing 1 µg/mL Hoechst dye for 10 minutes and then immediately imaged with the camera system described above.

Cells for mRNA isolation were trypsinized, spun down, washed with 1 mL of 1x PBS twice and resuspended in 100 µL of 1x PBS. Lysis buffer (Applied Biosystems, Carlsbad, CA), 100 µL, was added to the cells and briefly vortexed before storage at -20^{o}C. Total RNA was isolated in an RNA purification tray, using the ABI Prism 6100 Nucleic Acid Prepstation (Applied Biosystems, Carlsbad, CA) following the manufacture's protocol. Real-time RT-PCR amplifications were performed using a published protocol [93]. Single reactions with canine β-actin, Pax7, MyoD, Myogenin, and Utrophin (**Table 2.2)** were measured by the 7300 sequence detector in each well of a 96 well plate. Data analysis was done by ddCt method [94, 95].

Telomerase Expression

Telomerase expression experiments used the TeloTAAGGG Telomerase PCR ElisaPlus kit (Roche Diagnostics, Indianapolis, IN). Telomerase studies were conducted to determine the quantity of telomerase that is active in the isolated normal and GRMD cultures. Immortalized cell lines, HEK293 and C2C12, along with high and low control templates were used to determine relative telomerase activity (RTA). Samples were

processed per kit instuctions. PCR was done using a Verti 96 well PCR machine (Applied Biosystems, Carlsbad, CA) using the protocol provided with kit instructions.

Statistics

Results from biological samples, including immunohistochemistry, mRNA, cell fusion and relative telomerase activity were tabulated and error bars were calculated as standard error. P-values were calculated using a two-tailed students T-test.

Results

Cultures were visually indistinguishable between normal and GRMD dogs. These cultures consisted of small fairly rounded cells with one to three visible contacts with the cell culture plate. Small clusters of cells were seen after 2-3 days in culture. After three days in culture, cells would begin to elongate with two obvious points of connection and a few multinucleated cells would appear. Cultures of each genotype were put through the preplate procedure. More cells adhered to the culture plates from GRMD samples, especially in early preplates, presumably due to increased numbers of activated myoblasts, fibroblasts and macrophages. A portion of cells from preplates 5 and 6 were stained for desmin and Pax7 protein expression. In all cases the percentage of desmin positive cells was higher than the percentage of Pax7 positive cells (**Table 2.1)**.

Cells collected from each of the preplates, PP1-PP6 were subjected to mRNA analysis for the genes in **Table 2.2**. The later preplates showed elevated levels of all the myogenic associated genes for both normal and GRMD cultures (**Figure 2.1)**. GRMD and normal cultures had minimal expression of Pax7 and Myogenin in the early preplates, with expression rising in later preplates. GRMD cultures demonstrated low levels of

MyoD in early preplates and again rising levels in later preplates while normal cultures showed elevated levels of MyoD, ~40% of PP6, in the early preplates. Utrophin levels for both cultures started at about half that of the later preplates and increased in the later preplates.

Cultured cells were also analyzed for expression of NCAM-1 surface marker through FACS analysis. Approximately 85% of both normal and GRMD cells stained strongly for NCAM-1. Separate groups of cells also stained for CD45, the pan hematopoietic marker, and

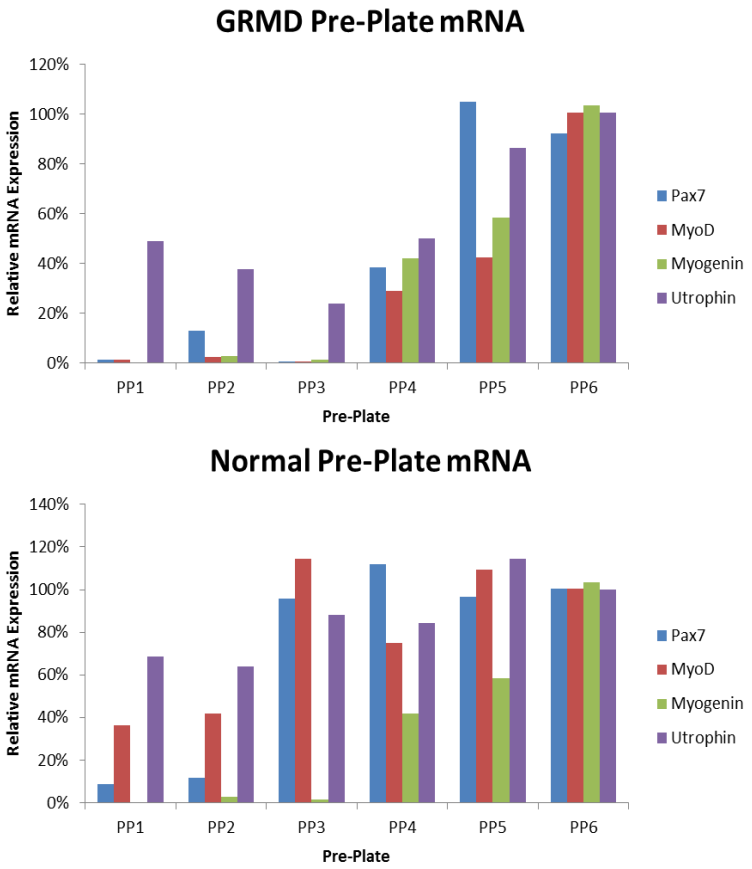

Figure 2.1. Preplate mRNA expression for Pax7, MyoD, Myogenin and Utrophin. Cells collected from passage 1 or 2. mRNA for genes of interest is relative to β-actin control mRNA.

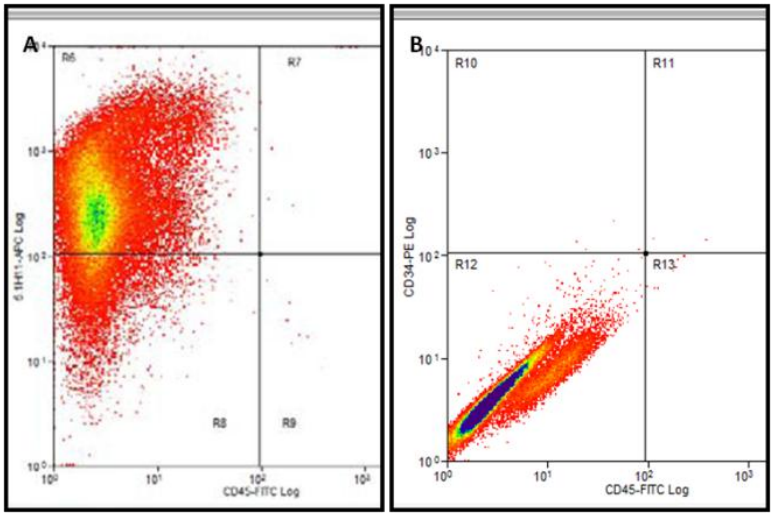

Figure 2.2. Flow cytometry of primary canine satellite cells and myoblasts. Cells are stained for A) NCAM1 and CD45 and B) CD34 and CD45. Cells are from a 4 month old normal dog and from preplates 5 and 6. X-axis CD45 (A & B); Y-Axis NCAM-1 (A), CD34 (B).

showed very little contamination with hematopoietic cells (**Figure 2.2 A & B)**. Cells showed no discernible expression of CD34 but were strongly positive for NCAM-1 (**Figure 2.2 B**).

Isolated cells were stained for myogenic associated proteins in growth and differentiation conditions, (**Figure 2.3)**. Transcription factors Pax7 and MyoD were readily visible in growth cultures. Myogenin, the transcription factor responsible for commitment to terminal differentiation, was only identified in rare nuclei in growth cultures but present in differentiation cultures on Days 3, 5, and 7. Desmin was seen in

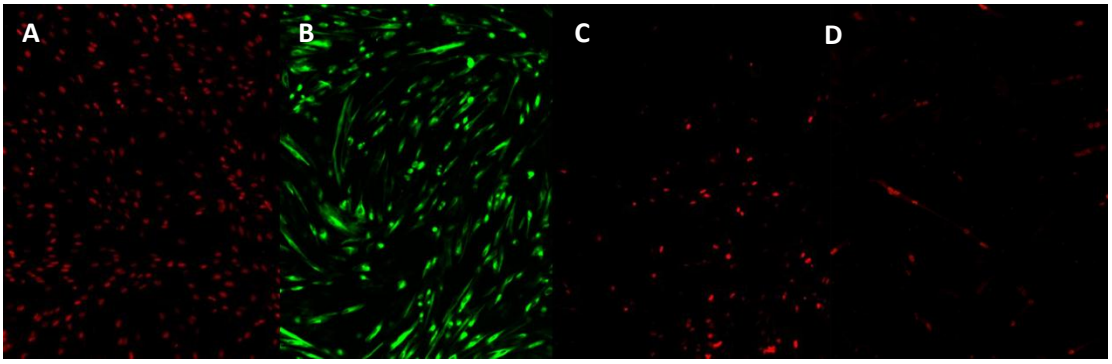

Figure 2.3 IHC for satellite cell and myoblast associated proteins. Pax7 growth (A), Desmin growth (B), MyoD growth (C), Myogenin differentiation (D). Cells are from preplates 5 and 6 from a normal dog. All images were taken with a 10x objective.

growth and differentiation cultures. Protein for the key myogenic factors Pax7, MyoD, and myogenin along with a terminal differentiation associated protein, myosin heavy chain, where quantified (**Figure 2.4)**. At Day 1, both normal and GRMD cultures had very similar numbers of nuclei expressing Pax7, MyoD, and myogenin and similar numbers of nuclei in cells that express myosin heavy chain.

From this point, normal and GRMD cultures began to diverge. Pax7 protein levels decrease and become significantly different ($p=0.03$) by Day 5, with normal cultures having a greater percentage of Pax7 positive nuclei **(Figure 2.4A)**. MyoD expression increased at Day 3 in both cultures but decreased from Day 3 to Day 5 in

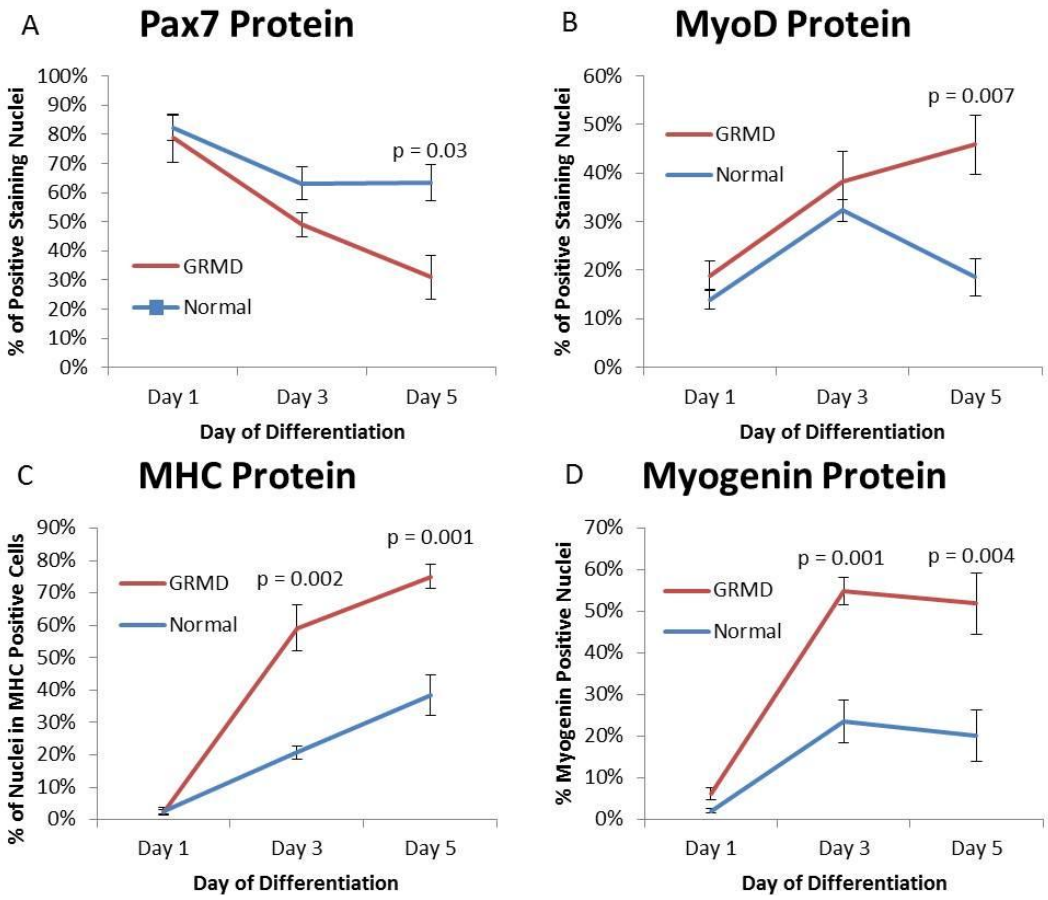

Figure 2.4. Percentage of nuclei expressing or associated with cells expressing myogenic proteins. Pax7 expression (A), MyoD (B), Myosin Heavy Chain (C), and Myogenin (D).

normal cultures while GRMD levels continued to increase at Day 5 (**Figure 2.4B)**. Positive MyoD nuclei percentage was significantly different on Day 5 (p=0.007).

MHC levels increased in both cultures over the 5 days but GRMD cultures showed a significantly greater number of nuclei associated with MHC positive cells on Day 3 (p=0.002) and Day 5 (p=0.001) (**Figure 2.4C)**. Myogenin levels also increased in both cultures over the 5 days where GRMD cultures showed a significantly greater number of positive nuclei on Day 3 (p=0.001) and Day 5 (p=0.004) (**Figure 2.4D)**.

The mRNA results of cultures derived from the late preplates, PP5 and PP6, of normal and GRMD samples showed that the late preplates express higher levels of myogenic associated mRNAs than early preplates, (**Figure 2.1)**. GRMD cultures showed

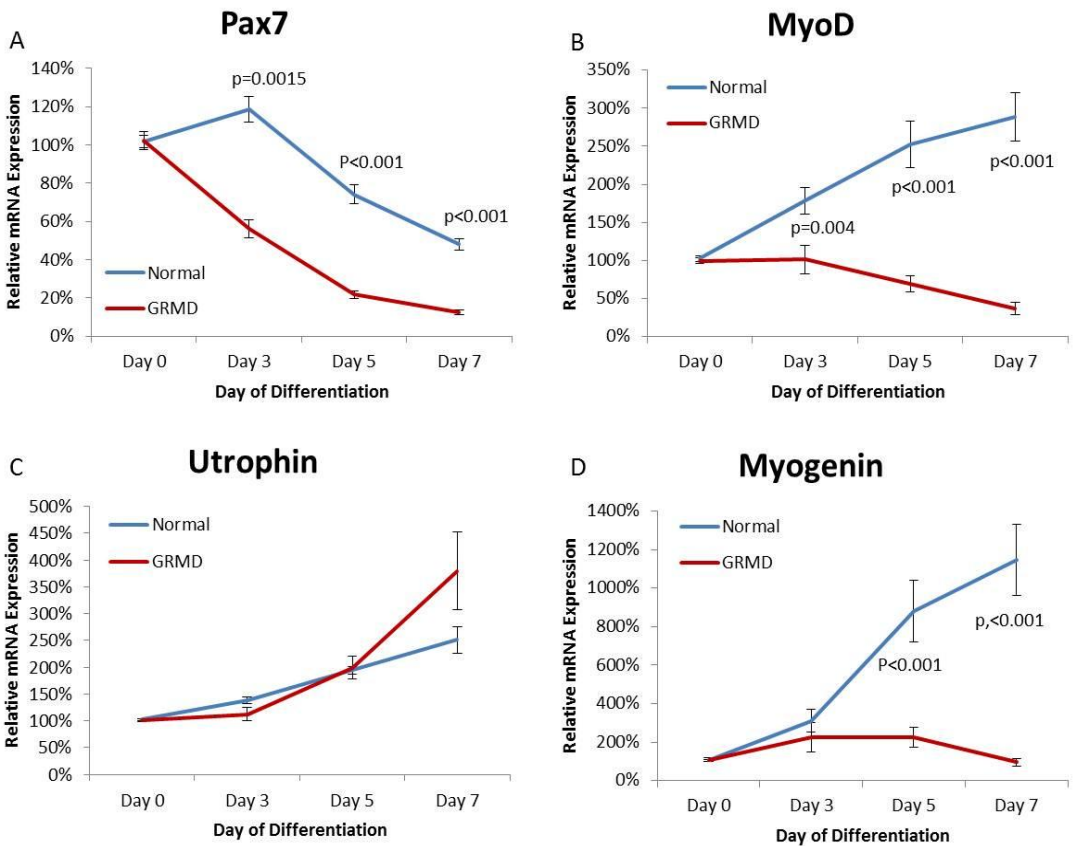

Figure 2.5. Relative mRNA expression for differentiation cultures. Cultures of normal and GRMD cells examined for Pax7 (A), MyoD (B), Utrophin (C), and Myogenin (D). Expression is measured against Day 0 mRNA levels, 100%, and followed for a 7 day differentiation. All expression is relative to β-actin mRNA internal controls.

very little myogenic associated mRNAs other than utrophin in there early preplates while normal samples showed higher levels of everything except myogenin.

Analysis of mRNA from cells isolated from normal and GRMD cultures, PP5 and PP6, that were collected in growth phase, Day 0, were indistinguishable between normal and GRMD samples for all of the mRNAs, (**Figure 2.5)**. Pax7 expression immediately dropped off between Day 0 and Day 3 for GRMD while normal cultures had an up-tick in expression. After Day 3, both cultures showed a decrease in Pax7 mRNA expression. From Day 3 to Day 7, normal Pax7 mRNA levels were significantly higher ($p<0.002$). MyoD expression was up-regulated in normal cultures while dropping off in GRMD

dogs, showing significant difference on Days 5 and 7 ($p<0.001$) (**Figure 2.5B)**. Utrophin mRNA expression levels increased similarly for both GRMD and normal samples through Day 7 but were not significantly different at any point (**Figure 2.5C)**.

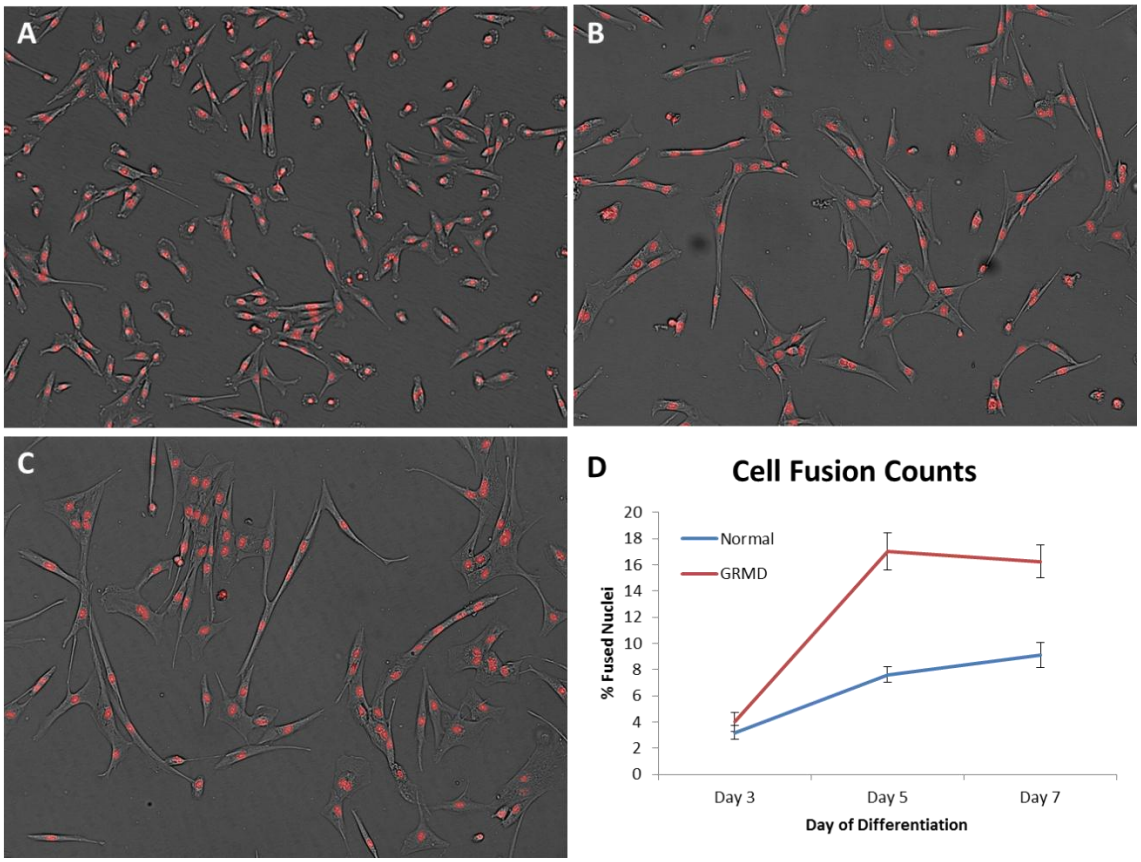

Figure 2.6. Cell fusion under differentiation. Nuclei (red) labeled with Hoechst dye and overlaid with brightfield images. Images taken at Days 3 (A), 5 (B), and 7 (C). Cells containing 3 or more fused nuclei quantitated and expressed as % Nuclei involved in cell fusions (D). Images taken with a 10× objective.

Myogenin mRNA was strongly up-regulated in normal cultures while GRMD cultures showed a relatively moderate increase through Day 5, followed by a decrease in expression by Day 7 (**Figure 2.5D).** Normal samples were significantly higher on Days 5 and 7 ($p<0.001$). Cell fusion studies showed that both normal and GRMD cells formed multinucleated myotubes (**Figure 2.6 A, B, & C)**. GRMD samples had a significantly greater ($p=0.004$) percentage of nuclei associated with myotubes on Days 5 and 7, ~17% for both days, than normal samples, ~8% for both days. GRMD cultures showed greater

capacity than normal cultures to form cell fusions at Day 5 and continuing through Day 7 (**Figure 2.6D)**.

Telomerase activity between normal and GRMD cultures was statistically indistinguishable (**Figure 2.7)**. RTA levels for all primary isolates were below the levels of the immortalized cell lines C2C12 and HEK293.

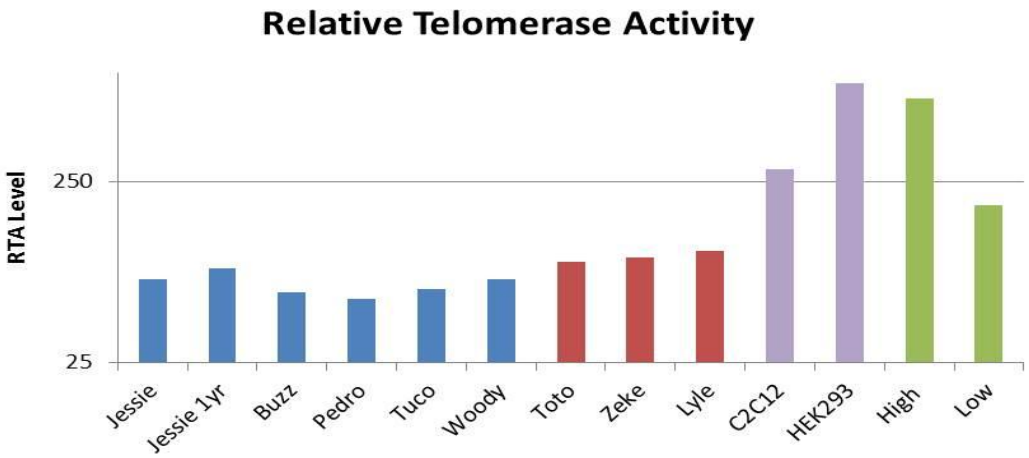

Figure 2.7. Relative telomerase activity in isolated primary cells and cell lines. Normal samples are in blue, GRMD samples in red, cell lines in violet and controls in green.

Discussion

The GRMD model is of great importance to the development and testing of therapies, whether they are pharmacological, genetic or cellular in makeup. Testing of cell-based therapies requires a more in-depth understanding of the cells that are primarily responsible for regenerating muscle, the satellite cells. Previous studies in dogs have found little if any difference between normal and diseased cultures of satellite cells [57, 85, 86]. Studies in mice have indicated that satellite cells isolated from the mdx model have a propensity to differentiate more quickly than their normal counterparts [92]. Published canine studies evaluated protein expression and growth rates to characterize

the cells. The characterization of these cells focused on the growth phase of cultures or at a single point at the end of the differentiation protocol. This provides some information on the basic character of the satellite cell, but there is more information to be found characterizing cells throughout the differentiation period at both the gene transcriptional and protein levels.

Our study evaluated the mRNA expression level of Pax7, MyoD, myogenin, and utrophin though a seven day differentiation period. We then characterized Pax7, MyoD, myogenin and myosin heavy chain expression with immunohistochemistry (IHC). Pax7 is a transcription factor known to be the master regulator of the satellite cell [34, 75, 96, 97]. Its expression inhibits the differentiation of satellite cells and myoblasts. MyoD is the second transcription factor and its expression is associated with activated satellite cells and proliferating myoblasts [54, 57, 78, 97]. MyoD expression follows that of Pax7 and is co-expressed for a time. Myogenin is one of several transcription factors associated with terminal differentiation of cells and the next transcription factor in this series [54, 77, 97]. Utrophin is a structural protein expressed in the cytosol of the cell [79]. Myosin heavy chain is also expressed during terminal differentiation and acts as a key component of the actin myosin network in functional muscle fibers [98].

Preplates from normal and GRMD dogs were analyzed for several transcription factors and utrophin expression at each of the preplate steps, PP1 to PP6 **(Figure 2.1)**. Expression of mRNA at each pre-plate, using the β-actin housekeeping gene as a control, was compared to PP6 levels, where the highest purity of satellite cells is expected [81, 83, 99]. The difference between the critical threshold of the β-actin and that of the gene of interest was the basis for analysis and comparison. Cultures for both normal and GRMD

showed low levels of Pax7, MyoD and myogenin in the early preplates, with these levels increasing in the later preplates, as expected. GRMD cultures had lower expression of the transcription factors in the early pre-plates than normal cultures. This could be due to larger amounts of other cell types found in GRMD biopsies, such as macrophages and fibroblasts[81]. Utrophin levels decreased slightly in GRMD samples from PP1 to PP3 and increased in the later preplates (**Figure 2.1)**. This could be due to cells in the biopsy undergoing terminal differentiation and expressing more utrophin at the time of isolation. These cells would also be strongly activated and "sticky" coming out in the early preplates.

Cells were also subjected to flow cytometry to assess purity of the cultures in regard to a surface marker, NCAM1, which has been used in the past to purify myoblast cell cultures. The level of NCAM1 expression on both normal and GRMD cultures was 85% with little contamination by macrophages as determined by CD45 co-staining (**Figure 2.2A)**. CD34 is known to be expressed on satellite cells but expression drops off in culture. These cultures showed very little expression of CD34 (**Figure 2.2B).** Purity of cells obtained via the preplate procedure is comparable to that obtained via flow cytometry for NCAM1, in previous studies [85].

Cultures were also evaluated for expression of Pax7, MyoD, Myogenin, and desmin protein using IHC. Desmin is a marker for myoblasts and newly formed myotubes but is not reliably expressed in satellite cells [83, 100]. Therefore, desmin is is not the best marker to determine the stem cell potential of a culture. However, its expression is still commonly determined to determine the purity of cultures. Pax7 is strongly expressed in satellite cells, regulating the stem cell state of these cells, and

serves as a better marker for the purity of cultures. This is especially true when considering cells to be used for transplantation purposes. Normal and GRMD cultures from late preplates, PP5 and PP6, were stained for desmin and Pax7. Desmin expression ranged from 100% to 88% expression in both cultures (**Table 2.1).** Pax7 expression was typically at 90 to 80%, with a range of 97% to 72% with. While the percentage of Pax7 positive cells was lower than those positive for desmin in all cases, . there were, no significant differences in percentages of cells expressing Pax7 were detected between normal and GRMD cultures in undifferentiated cultures.

Our studies provide static pictures of cells in a singular state just after isolation with the preplate procedure. However, satellite cells do not remain in a static state but instead respond to the environment and differentiate when called upon. Previous studies on mdx mice showed accelerated differentiation of mdx cultures looking at MyoD and myogenin protein expression under growth and differentiation conditions [92]. Studies of the changes in satellite cell regulation in vitro have not been reported before at the mRNA level. Examination of the transcription factors that regulate this process is needed to better characterize the GRMD model. Genes of interest were studied in cultures subjected to a differentiation procedure with low serum conditions carried out for seven days.

In the case of Pax7 mRNA, normal cultures showed a slight increase of the expression level, up to ~120% of levels before cells were subjected to a differentiation procedure. GRMD dogs did not demonstrate an increase in Pax7 mRNA levels. This can be seen at Day 3 in **Figure 2.5A**. From Day 3 to Day 7, expression levels decreased at

similar rates in both cultures. Normal cultures lost Pax7 mRNA expression before those from GRMD dogs.

MyoD mRNA expression was distinctly different over the course of the differentiation procedure in normal vs. GRMD cultures. Normal cultures show an up-regulation of the mRNA levels, to almost 300% of Day 0, while GRMD cultures showed a down regulation of MyoD expression, to around 35% of Day 0 (**Figure 2.5B)**. Since MyoD is associated with the proliferation of satellite cells and myoblasts and is lost when cells differentiate, it would be reasonable to conclude that the normal myogenic cells are continuing to proliferate while GRMD cells are undergoing more rapid differentiation.

Myogenin levels also increased in normal cultures over the preplates, while not changing in GRMD cultures (**Figure 2.5C)**. This is counter to the protein expression data where GRMD cells show a greater percentage of nuclei expressing myogenin, compared to normal cells, as the cells differentiate, (**Figure 2.4D)**.

Utrophin mRNA levels were similarly increased in both normal and GRMD cultures. Since utrophin expression not up regulated until fairly late in the differentiation cascade, relative to the previously noted transcription factors, it is not surprising that both cultures demonstrate similar levels of utrophin.

Our findings on mRNA levels were reinforced by the results from the changes observed in the percentages of cell expressing Pax7, MyoD, myogenin and MHC over a 5 day differentiation period (**Figure 2.4)**. On Day 1, percentages of nuclei positive for all of the transcription factors did not between normal and GRMD cultures. Percentages of nuclei found in cells expressing MHC were also indistinguishable between normal and GRMD cultures. The percentage of Pax7-positive nuclei decreased in both GRMD and

normal cultures (**Figure 2.4A)**. On Day 5, normal cultures had significantly higher expression percentages than GRMD cultures, pointing towards enhanced differentiation of GRMD cultures.

MyoD protein expression percentages increased in both normal and GRMD cultures to Day 3. By Day 5, normal cultures had lower levels and GRMD cell expression increased (**Figure 2.4B)**. Myogenin positive nuclei percentages started out around 2% on Day 1 with normal cultures increasing to 23% on Day 3. GRMD cultures had a much greater increase to 55% on Day 3, significantly more than normal cultures ($p=0.001$). By Day 5, both cultures maintained the percentages of nuclei expressing myogenin (**Figure 2.4D)**. Finally, MHC-associated nuclei started off low on Day 1 and increased on Days 3 and 5 for both cultures. Expression percentages for GRMD cultures were significantly higher on Days 3 and 5 (**Figure 2.4C)**. These results point toward an enhanced capacity of the GRMD cultures to differentiate even though growth phase cultures are indistinguishable between normal and GRMD cultures.

This propensity for greater differentiation can be seen in the results from cell fusion experiments (**Figure 2.6)**. Day 0 normal and GRMD cells were indistinguishable from one another. At Day 3, cells were noticed undergoing fusion events (**Figure 2.6A**). There was no difference between normal and GRMD cultures in the percentage of fused nuclei at Day3. However by Day 5, GRMD cultures demonstrated an increased number of fusion events over normal dogs ($p=0.003$) (**Figure 2.6D)**.

Early studies by Blau and colleagues utilizing isolation techniques demonstrated decreased numbers of satellite cells in mdx mice [87, 101]. However, in a subsequent study by this same group, similar numbers of Pax7 positive satellite cells were seen in

mdx and normal mice at 8 and 60 weeks [102]. These conflicting reports may have more to do with the methods used in isolation of cells rather than the disease state of the muscle. The 2010 study looked at the effect of telomerase deficiency on disease severity [102]. Cells that have undergone several rounds of cell division end up with shortened telomeres unless the telomerase enzyme is expressed in the cell. This allows cells to fall into a senescent state turning the mild mdx phenotype into a much more severe form of the disease. Reduced numbers of satellite cells were seen only in telomerase-deficient mice [102].

In the study conducted here, we assessed cells from young dogs, approximately four weeks of age, as this is the age at which cells for autologous cell modification and eventual therapy would be collected. Satellite cells should not be reduced in dystrophic muscle at this early age. Indeed, GRMD and normal cells expressed telomerase at similar levels (**Figure 2.7)**. This implies that GRMD cells are capable of maintaining the telomere length to a similar degree as normal cells, possibly preventing them from slipping into senescence. However, differences in telomerase activity might have been seen had samples from older GRMD dogs been evaluated.

Given these mRNA, protein, and cell fusion results, we conclude that GRMD cultures are in a more advanced differentiation state upon isolation from whole muscle tissue. Satellite cells and myoblasts may not have the time to become quiescent before again being activated, in the context of regenerating muscle. Satellite cells from normal and GRMD biopsies appear to be equivalently capable of proliferation but when subjected to differentiation, GRMD cells may have a greater propensity to differentiate.

As cells differentiate down the path to myotube formation, transcriptional and translational control of myogenic associated genes are altered. The cells isolated from the GRMD samples came out of tissue that has a larger number of activated satellite cells and myoblasts at various stages of differentiation, unlike normal satellite cells, which should be isolated at a quiescent stage. The layers of transcriptional control are likely altered in GRMD cultures to something downstream towards myotube formation when compared to normal cultures. Evidence for this can be seen in the altered mRNA transcript levels for the myogenic regulatory factors, Pax7, MyoD, and myogenin. Mechanisms for these differences are not completely understood and were not the subject of our studies.

These findings have implications for cell based therapies that would rely on isolating and manipulating the satellite cell population from GRMD dogs. Cells that are more prone to differentiate in culture may not be able to contribute to future myogenic repair of muscles as effectively as normal cells, leaving a need to continue the study of allogenic stem cell sources to repair and replace damaged and atrophying muscle tissue.

Chapter 3

Polystyrene-Coated Micropallets for Culture and Separation of Primary Muscle Cells

Introduction

Despite identification of a large number of adult stem cell types, current primary cell isolation and identification techniques yield heterogeneous samples, making detailed biological studies challenging. To identify subsets of isolated cells, technologies capable of simultaneous cell culture and cloning are necessary. Micropallet arrays, a new cloning platform for adherent cell types, hold great potential. However, the microstructures composing these arrays are fabricated from an epoxy photoresist 1002F, a growth surface unsuitable for many cell types. Optimization of the microstructures' surface properties was conducted for the culture of satellite cells, primary muscle cells for which improved cell isolation techniques are desired. A variety of surface materials were screened for satellite cell adhesion and proliferation and compared to their optimal substrate, gelatin-coated Petri dishes. A 1-μm thick, polystyrene copolymer was applied to the microstructures by contact-printing. A negatively charged copolymer of 5% acrylic acid in 95% styrene was found to be equivalent to the control Petri dishes for cell adhesion and proliferation. Cells cultured on control dishes and optimal copolymer-coated surfaces maintained an undifferentiated state and showed similar mRNA expression for two genes indicative of cell differentiation during a standard differentiation protocol. Experiments using additional contact-printed layers of extracellular matrix proteins collagen and gelatin showed no further improvements.

Polystyrene-coated micropallets for culture and separation of primary muscle cells.
Detwiler DA, Dobes NC, Sims CE, Kornegay JN, Allbritton NL.Anal Bioanal Chem. 2012 Jan;402(3):1083-91. Epub 2011 Dec 9.

Stem cells hold the promise of revolutionizing tissue engineering and other areas of regenerative medicine. Satellite cells, which are muscle progenitor cells, are a stem cell of great interest to the research community surrounding the family of diseases known as muscular dystrophy [2-5]. These diseases lead to a loss of muscle strength and/or function. The most severe form of muscular dystrophy, Duchenne muscular dystrophy (DMD), presents a progressive loss of strength in skeletal muscle and leads to muscle atrophy. Complications from progressive muscle deterioration limit the lifespan of affected individuals to two to three decades. Several animal models for DMD have been developed, with the two most influential being the mouse (MDX – muscular dystrophy X-linked) and the canine (GRMD - Golden retriever muscular dystrophy). The mouse model has been used extensively to examine the underlying disease physiology [6, 7]. The canine model, GRMD, better mimics the human disease in severity and is a size relevant model [8, 9]. Currently there are no clinically available therapies that correct, halt or limit the progression of the disease, though clinical trials are underway [10-12].

One therapeutic approach to treat DMD uses transplantation of satellite cells to correct or replace the cells responsible for muscle tissue regeneration. This approach, in principle, has the ability to restore lost muscle mass in late-stage patients. Currently, techniques to isolate and purify satellite cells and other muscle progenitor cells such as myoblasts have been based primarily on the preplate method and flow cytometry. The preplate technique is based on the adhesion of cells to polystyrene tissue culture dishes and involves repeated decanting and culture of the supernatant [80, 81]. Quiescent

satellite cells become activated only after a stimulus signals the need to repair damage. Thus in the initial platings, these cells are non-adherent and remain in the supernatant. Other undesired cell types, such as fibroblasts and macrophages, are programmed to actively perform functions within the muscle and adhere rapidly to polystyrene, remaining on the surface during the initial platings [65, 81]. This preplating technique ultimately results in a satellite-cell-enriched but nonetheless heterogeneous mixture of cells.

Alternatively, flow cytometry protocols are capable of generating populations of increased purity, but require functional antibodies specific to cell surface markers. Particularly for canine cells, which at present lack an adequate repertoire of antibodies for selection, the technique's ability to sort and purify the desired cells remains limited and requires further cell characterization. Thus, new technologies are needed to more effectively sort and purify primary canine satellite cells (PCSCs).

The advent of microfabricated devices has enabled novel investigations of biological properties. Micropallet arrays have provided a means to clonally culture and isolate cells based on a wide range of characteristics, including the presence or absence of fluorescently tagged proteins, and additional criteria not available to flow cytometry, including cell morphology, growth rate, and other dynamic behaviors [58, 60]. With the large number of microstructures available on an array, the cloning and isolation of moderate to large numbers of cells is greatly simplified over standard tissue culture cloning techniques. Micropallet arrays have previously been used to clone and sort tumor cells, murine embryonic stem cells, and other cell lines [58, 60, 62, 63]. While numerous generations of these cell lines have been adapted to cell culture conditions, more

physiologically relevant primary cells are not so adept at adhesion to artificial surfaces. This creates the need for a tailored culture surface to meet the requirements of these primary cells.

In this research, we have optimized the surface of micropallets for PCSCs, the cells responsible for maintenance and regeneration of skeletal muscle. Contact printing of the micropallets was evaluated for its capacity to generate a suitable surface for the culture of PCSCs and to lay the groundwork for developing procedures applicable to other primary cell types [62, 64, 103]. The long-term goal of this work is to utilize the micropallet arrays to sort PCSCs using a variety of parameters and shorter timescales not available through traditional cloning techniques or flow cytometry. This is expected to enable more efficient characterization of these cell types than is currently possible, as well as identify new cell subsets not previously identified.

Materials and Methods

Polymer and Copolymer Synthesis

Various polymers were synthesized, including neutral polystyrene (PS) and positive and negative copolymers. Briefly, components (**Table 3.1)** were weighed and

Copolymer Type	Toluene	Styrene	Acrylic Acid	Dibenzoyl Peroxide	4-Vinyl-Pyridine
Neutral	69.8%	29.9%	-	0.3%	-
11% 4VP in PS	67.6%	29.0%	-	0.3%	3.1%
2.5% AA in PS	69.8%	29.2%	0.7%	0.3%	-
5.0% AA in PS	69.8%	28.4%	1.5%	0.3%	-
10% AA in PS	69.8%	26.9%	3.0%	0.3%	-
15% AA in PS	69.8%	25.4%	4.5%	0.3%	-
20% AA in PS	69.8%	23.9%	6.0%	0.3%	-

Table 3.1 Composition of copolymers by wt%

mixed in a fume hood and placed in a 60 °C water bath overnight to polymerize. Negatively charged copolymers containing > 2.5% acrylic acid (AA) precipitated out of the toluene solvent forming a solid layer on the bottom of the reaction vessel. After reactions using these concentrations and polymers, the remaining solvent was decanted and replaced with an equal amount of tetrahydrofuran (THF) (Sigma, St Louis, MO) to solubilize the copolymer. For the 2.5% AA in PS copolymer, only a partial copolymer layer precipitated from the toluene, thus the toluene was evaporated from the mixture on a 60 °C hotplate to recover any non-precipitated copolymer. Once the toluene was removed, an equal volume of THF was added to dissolve the 2.5% AA in PS copolymer completely. Positively charged copolymers containing 4-vinyl pyridine (4VP) were fully soluble in toluene, so replacing toluene with THF was not necessary.

Cell Isolations and Culture

PCSCs were isolated from muscle biopsies of the vastus lateralis of a normal dog in the GRMD colony at University of North Carolina at Chapel Hill (UNC-CH). Cells were isolated from biopsies as previously described with minor modifications [65, 81]. Briefly, biopsy material was finely minced and digested with collagenase in growth media, 16.5% FBS in Dulbecco's Modified Eagle Media (DMEM), for 6-8 h. Material was rinsed and digested with 0.05% trypsin for 1 hr with agitation every 15 min. Material was then passed through a 100 μm screen followed by a 40 μm screen and plated on 0.1% gelatin (Millipore, Billerica, MA) coated tissue-culture-treated polystyrene (TC) Petri dishes (BD Falcon, Franklin Lakes, NJ). Six successive platings with the preplate procedure resulted in enriched populations of PCSCs, with cells from plates 4, 5, or 6

used in the current experiments [81, 99]. To confirm the presence of PCSCs, 1000 cells from passage two of preplate 5 were fixed and stained with anti-desmin antibodies and counterstained with Hoechst dye. Desmin, a marker for PCSC, was detected in 94% of the cells. The enriched cell populations were further cultured in uncoated TC dishes in 16.5% fetal bovine serum in Dulbecco's Modified Eagle Medium (DMEM), with 1% penicillin-streptomycin defined as standard growth conditions [55]. To differentiate the PCSCs, the cells were cultured in 2% horse serum (Invitrogen, Carlsbad, CA) in DMEM with 1% penicillin-streptomycin, defined as standard differentiation conditions [55].

Photoresist and Polymer Film Fabrication

Photoresist, 1002F, was prepared as previously described (see also **Figure 3.1A**) [104]. Approximately 1.5 mL of 1002F was poured into the center of a plasma-cleaned glass slide (75 × 25 × 1 mm, Corning, Corning, NY). The photoresist was spin-coated onto the slides by spinning at

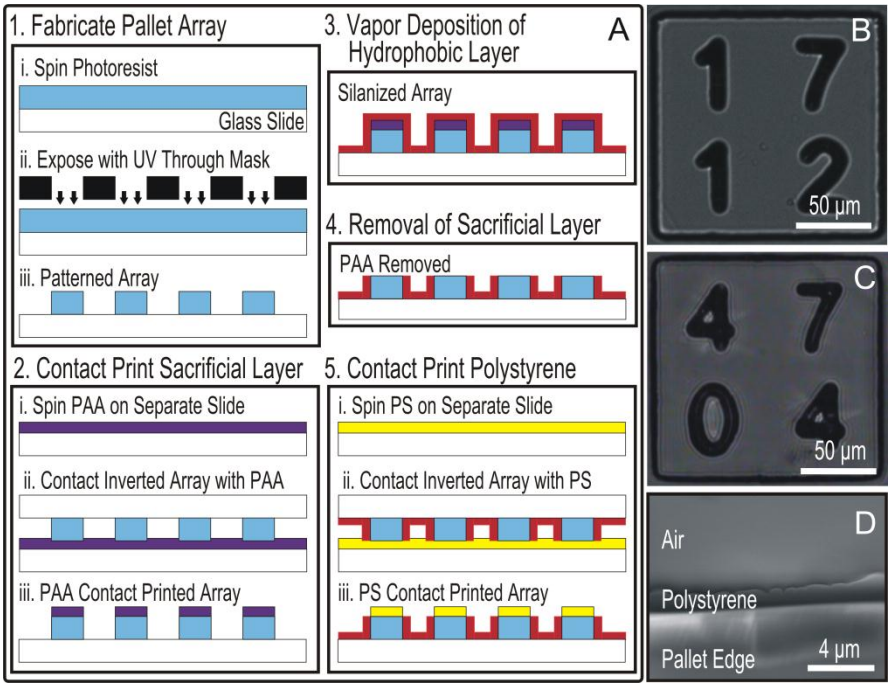

Figure 3.1. Pallet array fabrication. a) Schematic showing patterning of array (step 1), poly(acrylic) acid (PAA) contact printing (step 2), deposition of hydrophobic silane layer (step 3), Removal of PAA layer (step 4), and polystyrene-copolymer contact-printing (step 5). b) Brightfield image of pallet with no coating. c) Brightfield image of pallet contact-printed with 5% AA in PS. d) ESEM image of pallet viewed on edge showing polystyrene thickness.

500 rpm for 10 s, followed by 2200 rpm for 30 s. Photoresist, coated on glass slides, was placed in a 95 °C oven (Fisher Scientific, Dubuque, IA) for a 50 min soft bake, removed and allowed to cool to room temp. Soft baked photoresist was placed on a UV exposure system (Oriel, Newport Stratford, Inc., Stratford, CT) and illuminated with 1500 mJ. Exposed photoresist was returned to the 95 °C oven for a 10 min post-exposure bake (PEB), removed and permitted to cool to room temp. PEB-photoresist was placed in a photoresist developer (1-methoxy-2-propyl acetate, Sigma-Aldrich, St. Louis, MO) on a rotary shaker for 4 min. Developed photoresist was rinsed with 2-propanol (VWR, West Chester, PA), blown dry with nitrogen, and placed on a hotplate at 95 °C for 10 min, followed by 70 min at 120 °C. To add the polystyrene film, room temp photoresist films were again placed on the spin coater, coated with 3 mL of the desired polystyrene by spinning at 500 rpm for 10 s. Polystyrene-coated photoresist films were then placed in a 60 °C vacuum oven (VWR, West Chester, PA) for at least 48 h to evaporate any remaining solvent.

Micropallet Array Fabrication and Contact Printing of Polystyrene and Extracellular Matrices (ECMs)

Micropallet arrays were fabricated as previously described (see also **Figure 3.1A**) [58, 104]. Briefly, a mask outlining numbered micropallets was used to photolithographically define a 50 × 50 array of 150 × 150 × 50 μm (L x W x H) micropallets possessing a 50 μm gap between micropallets. Polyacrylic acid (PAA) (Polysciences Inc., Warrington, PA), 25% in aqueous solution (MW:~50,000) diluted to 8% in DI water, was applied to the upper micropallet surfaces via contact printing [64].

This deposited PAA would serve later as a sacrificial layer to remove the organosilane ([heptadecafluoro-1,1', 2, 2'-tetrahydrodecyl] trichlorosilane, Gelest, Morrisville, PA) from the top surface of the micropallets. Only arrays possessing ≥90% fully PAA-coated micropallets were used in subsequent steps. Approximately 80% of the arrays met this criterion. The organosilane was applied by vapor-deposition in a vacuum chamber as previously described [58]. Arrays were removed from the chamber, incubated in deionized water for 30 min and rinsed with deionized water to remove the sacrificial PAA layer. Micropallet surfaces were then contact-printed with the desired polystyrene coatings (**Table 3.2)**,again only using arrays possessing ≥90% fully polystyrene-coated micropallets in subsequent steps [64]. Again, approximately 80% of the arrays met this criterion. Once printed with polystyrene, arrays were placed in a 60 °C vacuum oven for

PS Type	Spin Speed (RPM)	Time (sec)	Volume (mL)	Dilution (PS:THF)
Neutral PS	500	10	1	None
11% 4VP in PS	1000	11	1	None
2.5% AA in PS	400	5	2	None
5.0% AA in PS	400	5	2	None
10% AA in PS	400	5	2	1:1
15% AA in PS	400	5	2	1:2
20% AA in PS	300	5	2	1:4

Table 3.2. Optimized parameters for contact printing various copolymers onto 1002F surfaces.

48 h to remove any remaining solvent. Arrays were sterilized with 75% ethanol and allowed 30 min to dry.

To contact-print ECMs, 5 μL of 1 mg/mL collagen or 3 μL of 1 mg/mL gelatin was added to a sterile glass slide and spread with the side edge of a pipette tip to cover a 1 cm^2 area. Arrays were then inverted and pressed against the protein-coated slide and removed to create a single-layer coating. This procedure was repeated to create a double-

layer coating. In experiments to determine the persistence of the gelatin layer contact printing, gelatin was labeled with a fluorescent Alexa Fluor®568 (Invitrogen, Carlsbad, CA) per manufacturer protocol. Labeled gelatin was printed in two layers onto the micropallets, allowed to dry, placed in standard growth conditions and imaged. Cells were plated onto the array and images were taken again at 24 and 96 h.

Measuring Contact-Printed PAA and Copolymer Thickness

Micropallets contact-printed with copolymers were observed using an environmental scanning electron microscope (ESEM) (Quanta 200, FEI Company, Hillsboro, OR). The ESEM was performed in low vacuum (0.75 Torr) mode and a backscattered electron detector was used to acquire images. Contact-printed micropallets were also removed from the glass surface and imaged from the side (**Figure 3.1D**). The thickness of the contacted-printed copolymer layer, in addition to the thickness of the contact-printed PAA layer, was measured using a profilometer (P6 Stylus Profilometer, KLA Tencor, San Jose, CA). Copolymer and PAA thickness were determined by measuring micropallet height before and after contact-printing.

Experiments Studying Cell Adherence and Proliferation

Cell chambers were created from poly(dimethylsiloxane) (PDMS) reservoirs (10 × 10 × 8 mm) glued with uncured PDMS onto the 1002F and copolymer films or micropallet arrays. Before use, the cell chambers were sterilized with 75% ethanol and allowed to dry 30 min in a tissue culture hood under sterile conditions. Reservoirs were rinsed twice with 1 mL of phosphate buffered saline (PBS). Before seeding cells, 500 μL of media was added and allowed to sit for 10 min. Cells were then loaded into the reservoir as 500 μL of an 8000 cells/mL suspension added drop wise into the reservoir in

a grid-like pattern to spread the cells evenly over the array. Cells were then placed in a 37 °C incubator (5% CO_2, ~95% RH) for up to 96 h during the course of the experiment.

Cell Imaging and Counting

Cells grown on films of copolymer, photoresist, or micropallet arrays were stained with 1 μg/mL Hoechst 33342 (Sigma, St. Louis, MO) for 10 min in a 37 °C incubator. Cells were imaged with an epifluorescence microscope (IX81, Olympus, Center Valley, PA) using a Coolsnap HQ^2 charged coupled device camera (Photometrics, Tucson, AZ). For cells on films, six independent images were obtained at 4× magnification, and cells were counted using ImageJ software (NIH, Bethesda, MD). Cells grown on micropallet surfaces were imaged at 10× and the numbers of cells per micropallet were counted using a Matlab script (Mathworks, Natick, MA).

mRNA Analysis

Four aliquots of 150,000 cells were placed in 1.5 mL microcentrifuge tubes. Tubes were centrifuged at 600 g for 2.5 min and media was then removed, leaving the cell pellet. Pellets were rinsed with 1 mL of 1× PBS and centrifuged again. The supernatant was removed leaving the cell pellet in 100 μL PBS. A 100 μL quantity of 2× nucleic acid lysis buffer (Applied Biosystems, Carlsbad, CA) was then added to the tube. The suspension was mixed and placed in a -20 °C freezer. These tubes were denoted as Day 0. Additional aliquots of cells were plated on the experimental surfaces as follows. Glass slides (75 × 25 × 1 mm) were coated with 1002F photoresist and 5% AA in PS films as described above and PDMS reservoirs were applied. Samples were sterilized with ethanol and rinsed with PBS, followed by 4 mL of warmed growth media. A cell suspension (37,500 cells/mL, 2 mL) was added drop wise to each plate, applied in a grid-

like pattern. Plates were then placed in a 37 °C incubator (5% CO_2, ~95% RH). On Days 3, 5, and 7, cells were collected for analysis. To collect, samples were rinsed with PBS and cells were removed with 500 μL of trypsin-EDTA (Invitrogen, Carlsbad, CA) followed by addition of 500 μL of PBS. Samples were then prepared in the same fashion as Day 0. Once all trials were complete, samples were submitted to the UNC-CH Animal Clinical Chemistry and Gene Expression Laboratories for RNA analysis using TaqMan® probes on an ABI PRISM® 770 Sequence Detection System (Applied Biosystems, Carlsbad, CA) using primer probe sequences developed for *Pax7* and *Utrophin*. *Pax7* primers/probe: Forward (AGT ACG GCC AGA CTG CTG TT), Reverse (AAT GCT CCC CGA GCT TCA TA), Probe (Fam AC CTG GCC AAA AAC GTG AGC CTC TCTamra). *Utrophin* primers/probe: Forward (CTG ACA GCA GCT CTA CCA CA), Reverse (CCT CCA AGC GTC TGA CAG TA), Probe (Fam TG TGG AGG ACG AGC ATG CCC TCA TC Tamra).

PCSC Separation and Pax7 Verification

A heterogeneous population of cells derived from a muscle biopsy was obtained from the earlier stages of the preplate procedure described above, specifically preplate 4. 2000 cells were seeded onto an array of 2500 micropallets of dimensions 150 × 150 × 50 μm (L×W×H). Cells were allowed 48 hrs to adhere and micropallets were examined for cellular adhesion. Micropallets containing cells with a spindle-like morphology were released from their glass substrate using an ACL-1 532 nm frequency-doubled Q-switched Nd:YAG laser (New Wave Research, Fremont, CA) generating ~7 μJ laser pulses with a 5 ns pulse width as previously described with minor modifications [58]. The glass slide containing micropallets was placed inverted atop a 15 × 15 × 4 mm

PDMS reservoir affixed to a glass slide containing culture media (described above). The laser was focused at the base of the micropallet through a Nikon Eclipse E800 upright microscope (Nikon, Melville, NY) using a Nikon 20× extra-long working distance objective (Nikon, Melville, NY). The microscope was fully enclosed in a 37°C incubated environment with humidity and temperature controls provided by an Air-Therm ATX-H Controller (World Precision Instruments, Sarasota, FL) and CO_2 control provided by a ProCO2 Controller (Biospherix, Lacona, NY) (4% CO_2, ~75% humidity). After being released into the media-filled tissue culture dish, cells were placed in a 37°C incubator (5% CO_2, ~95% RH) and allowed to proliferate for 48 hrs. After this time, cells were stained via a modified protocol for the transcription factor and intracellular marker Pax7 [57, 75]. Briefly, cells were rinsed in PBS and fixed in a 4% paraformaldehyde solution in PBS for 10 min. Cells were permeablized for 15 min with 0.5% Triton X-100™ in PBS to permit antibody access to the nucleus. Primary mouse anti-Pax7 antibody (DSHB, Iowa City, IA) used at 2µg per mL was incubated on cells for 12 hrs. Secondary anti-mouse antibody labeled with AlexaFluor®594 (Invitrogen, Carlsbad, CA) was incubated at 4µg per mL on cells for 1 hr. Cells were imaged with the previously described epifluorescence microscope using DAPI and Texas Red filters (Olympus, Center Valley, PA).

Results and Discussion

Surface Modifications for Growth of PCSCs

The 1002F photoresist from which the micropallet arrays were fabricated has been shown to be suitable for culturing tumor cell lines [58, 62]. In some instances, the

1002F required an additional coating such as collagen or fibronectin for cell attachment and growth. When PCSCs were cultured on the arrays, cells initially adhered to the 1002F surface, but did not proliferate. The addition of an adsorbed ECM to the micropallet surfaces also failed to support cell proliferation. The 1002F beneath the ECM may have leached a component toxic to the overlying cells or the ECM may not have exhibit the same properties as those on the polystyrene surfaces of tissue culture dishes. For this reason, a variety of surface coatings designed to mimic either the glass or polystyrene culture surfaces on which these cells are traditionally grown were placed onto the arrays. Layers of microbeads (22 nm and 500 nm silica glass or 50 nm polystyrene) contact-printed on to the array surfaces exhibited a non-uniform coating, with cracking of the printed layer and surface-detachment after 4 days. [64]. Since these defects were not compatible with light microscopy and may have also permitted leached materials from the 1002F to contact the cells, these modifications were not tested further.

Polystyrene is a standard and well-accepted surface for cell culture; therefore, polystyrene in an organic solvent was contact-printed onto the micropallets [19]. The polystyrene layer exhibited a uniform surface coverage, unambiguous transparency, and no visible cracking, **Figure 3.1B, C**. The coating also remained on the micropallet surface for two weeks in culture, the maximum time examined, making the contact-printing of thin layers of polystyrene a convenient method of modifying micropallet surfaces for microscopy applications.

Standard TC dishes are the accepted culture vessel for PCSCs, and were therefore used as the gold standard for comparison of cell adhesion and proliferation [81, 99]. Commercial TC dishes are oxidized, imparting a negative charge to the surface [105,

106]. Direct oxidation of the polystyrene-coated micropallet surfaces was not possible since the hydrophobic organosilane coating on the intervening glass surface was not stable to oxidants. This hydrophobic coating is used to entrap air between the micropallets, blocking cell access to the inter-pallet regions. Since these virtual air walls are critical to direct cells to the micropallet surfaces, another strategy was required to impart a charge to the polystyrene coating. For this reason, the charged monomers acrylic acid (negative charge) or 4VP (positive charge), were mixed into the styrene monomer at different concentrations during polymer synthesis to form polystyrene copolymers with varying charge densities. To determine whether PCSCs could be cultured on these polymers, flat films comprised of the copolymers were assessed for PCSC adherence and growth over 4 days, **Figure 3.2**. PCSCs did not efficiently adhere to or proliferate on the uncharged polystyrene or the 4VP in polystyrene. Negatively charged copolymers of acrylic acid in polystyrene (AA in PS) supported greater cell adhesion and proliferation than any of the other synthesized surfaces at all time-points. Within the first 24 h, the negatively charged AA-in-PS coating showed no significant differences for any AA concentration

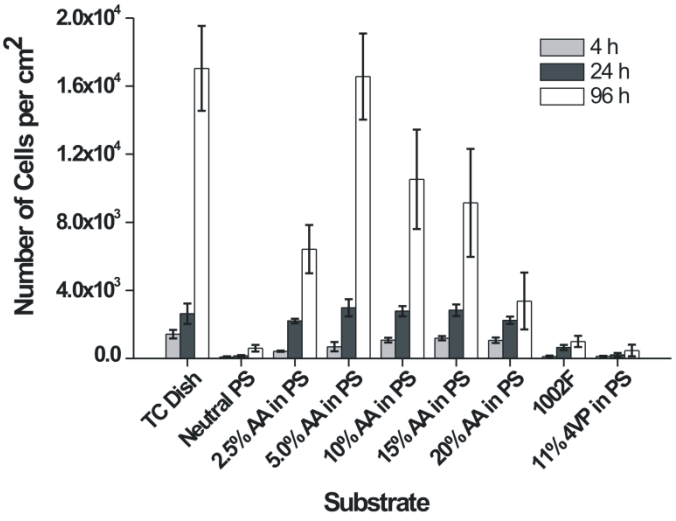

Figure 3.2. Cell adhesion and proliferation on various thin film substrates. PCSCs purified with the preplate technique were cultured on TC dishes, neutral PS, various percentages of AA in PS, 1002F photoresist (1002F), or 4VP in PS. Cells were stained with Hoechst dye, imaged and counted at 4, 24 and 96 hours.

when compared to standard TC dishes. However, by 96 h, PCSCs on the 5% AA-in-PS surface exhibited equivalent growth properties to that on the TC dish. In contrast, the surfaces with 2.5, 10, 15 and 20% AA in PS demonstrated significantly lower rates of proliferation as revealed by the lower cell numbers at 96 h. Cells grown on the TC dish and 5% AA in PS showed similar morphology, long slender cells, **Figure 3.3**. Cells grown on the bare 1002F were scattered and more rounded in morphology. These data demonstrated that PCSCs adhere to and proliferate on the 5% AA in PS copolymer as

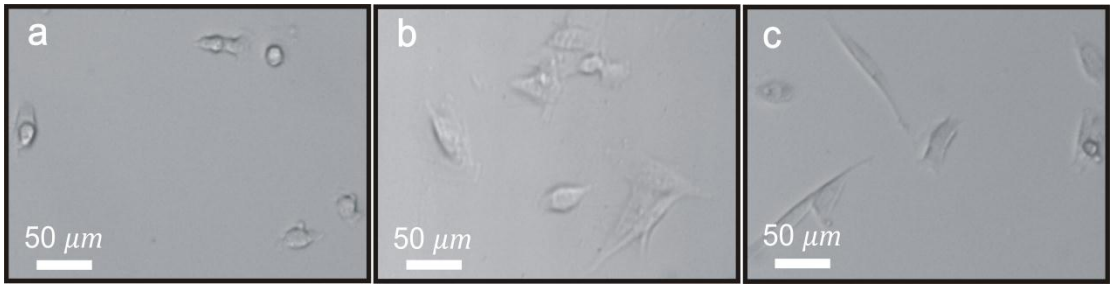

Figure 3.3. PCSCs cultured on various surfaces. a) bare 1002F photoresist film, b) photoresist film coated with 5% AA in PS and c) TCPS. Magnified images of PCSCs grown on these surfaces are

effectively as on the "gold standard" surface of the TC dish, making 5% AA in PS atop 1002F micropallets an effective growth surface for these primary cells.

Characterization of Contact-Printed PAA and Copolymer

To determine the thickness of the 5% AA-in-PS layer contact printed on to the micropallets, ESEM was used to image individual micropallets. The apparent polymer thickness was 1-2 μm, **Figure 3.1D**. Since the exact orientation of the pallet was difficult to ascertain, more precise measurements of the layer thickness could not be obtained using ESEM. For a more precise measurement, a stylus profilometer was used to measure the height of the micropallet above the glass substrate before and after contact printing with 5% AA in PS. The same procedure was completed for the contact-printed PAA. The

copolymer thickness was 1.0 μm ± 0.3 μm (n=50), while the PAA thickness was 0.63 μm ± 0.2 μm (n=50).

ECM Protein Coatings

PCSCs are commonly cultured on collagen or gelatin-coated TC flasks [81, 99]. For this reason, gelatin was contact-printed onto the surface of the micropallet arrays composed of 1002F micropallets with a 5% AA in PS top layer. To determine whether the contact-printed gelatin was stable over time, AlexaFluor®568-labeled gelatin was utilized and two layers of fluorescent gelatin were contact-printed onto the array. Arrays with or without cultured cells were incubated for 4 days under standard tissue culture conditions. Images were taken immediately after the adhesion of cells at 4 h and again at 24 and 96 h. The gelatin fluorescence intensity on the micropallets decreased from 1.00 at 4 h to 0.90 ± 0.05 at 24 h. The fluorescence intensity then remained unchanged through 96 h, indicating that the gelatin remained attached to the surface of the pallet for the duration of the culture period. Pallets contact-printed with fluorescent gelatin and cultured with cells also demonstrated a drop in fluorescence from 1.00 at 4 h to 0.90 ± 0.11 at 24 h. The fluorescence intensity was then unchanged through 96 h. In this instance the fluorescence of the cell's cytoplasm plus that of the micropallet surface was measured since the two fluorescence sources could not be separated. Cells growing on the gelatin demonstrated bright red punctate spots suggesting that they were able to take up the fluorescent dye. This phenomenon was most likely due to the enzymatic degradation of the fluorescent gelatin by the cells and subsequent uptake of the labeled protein [107].

Cells on 5% AA-in-PS-coated micropallets with either a single or double layer of contact-printed gelatin did not demonstrate significant enhancement in initial cell adhesion or proliferation compared to those on the 5% AA-in-PS-coated micropallet alone, **Figure 3.4A&B**. Similar results were obtained when collagen was contact-printed onto micropallets in either single or double layers. These data suggested that the ECM coating was not necessary for PCSC adherence and growth on the micropallets containing a 5% AA-in-PS surface.

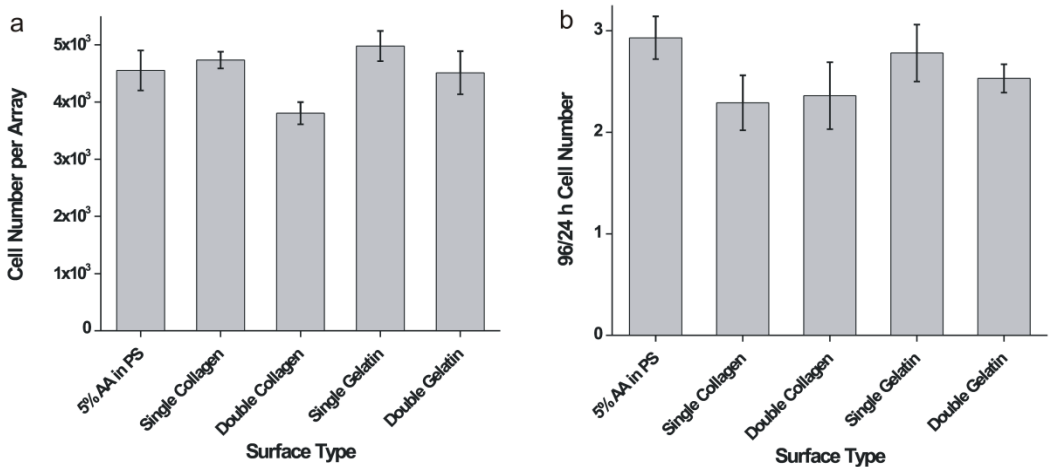

Figure 3.4. Adhesion and proliferation of cells on micropallets contact-printed with selected proteins. a) Number of PCSCs adhering at 24 hours to micropallet arrays contact-printed with 5% AA in PS alone, with 5% AA in PS followed by contact printing with collagen or gelatin (single) or with 5% AA in PS gelatin followed by two-sequential, contact printings with collagen or gelatin (double). b) Ratio of the number of PCSCs counted at 96 hours to 24 hours on micropallet arrays contact-printed with 5% AA in PS alone or with an additional single or double layer of collagen or gelatin. Micropallet arrays for both (a) and (b) consisted of 2500 micropallets of dimensions 150 µm × 150 µm× 50 µm (L × W × H).

Monitoring Growth and Differentiation of PCSCs on Standard and Optimized Surfaces

A risk in culturing cells on novel surfaces is the potential to alter cellular properties, such as the induction of PCSC differentiation toward terminally differentiated multi-nucleated myotubes [55, 108-110]. This process is regulated by the transcription

factor Pax7, which maintains the stem cell state. Utrophin, a structural protein, is indicative of PCSC differentiation [78, 79]. Differentiation patterns of the PCSCs cultured on commercial tissue culture dishes versus films composed of the 5% AA in PS were assayed for their ability to remain undifferentiated as well as their ability to respond to a differentiation signal. The relative mRNA expression levels of *Pax7* and *Utrophin* corresponding to undifferentiated and differentiated states, respectively, were measured [56, 78, 79, 97, 111]. Under standard growth conditions, cells cultured on 5% AA in PS and TC dishes remain undifferentiated, maintaining relatively high stable mRNA levels of *Pax7*, **Figure 3.5A**, and low levels of *Utrophin*, **Figure 3.5B** [55]. When subjected to standard differentiation conditions (addition of horse serum), the rate of differentiation of PCSCs was similar on both 5% AA-in-PS surfaces and TC dishes, as shown by a decrease in *Pax7* mRNA quantity over time, **Figure 3.5A,** and an increase in *Utrophin* mRNA levels over time, **Figure 3.5B** [55]. The samples cultured on the TC dishes or the 5% AA-in-PS surfaces under either the standard growth or differentiation conditions did

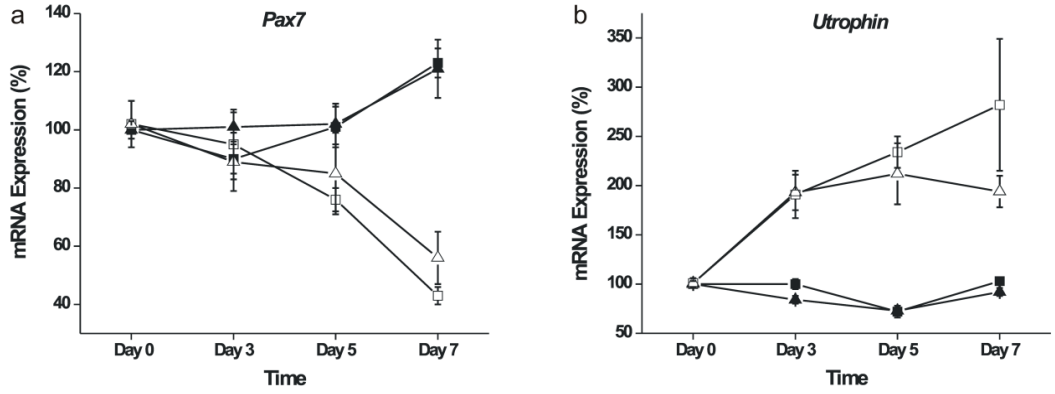

Figure 3.5 mRNA expression levels under standard growth and differentiation conditions. a) *Pax7* mRNA expression in PCSCs grown on TC dishes (squares) or 5% AA in PS-coated films (triangles) in either standard growth (solid symbols) or differentiation (open symbols) conditions. b) *Utrophin* mRNA expression in PCSCs grown on TC dishes (squares) or 5% AA in PS (triangles) in either standard growth (solid symbols) or differentiation (open symbols) conditions. For both (a) and (b) mRNA expression levels are normalized to Day 0.

not demonstrate statistically distinct mRNA levels of *Pax7* or *Utrophin* using a one tailed student T-test.

PCSC Separation and Pax7 Verification

Satellite cells have been demonstrated to grow with a spindle-like morphology in culture (characterized by two to three points of attachment) [67, 88]. Satellite cells also express the transcription factor and internal marker, Pax7 [57, 75]. A brief separation and verification experiment was devised to demonstrate this correlation. Micropallet arrays coated with 5% AA in PS were seeded with a heterogeneous mixture of cells from a canine muscle biopsy subjected to the preplate procedure [83]. Micropallets containing cells with a spindle-like morphology were identified and released from the array onto a

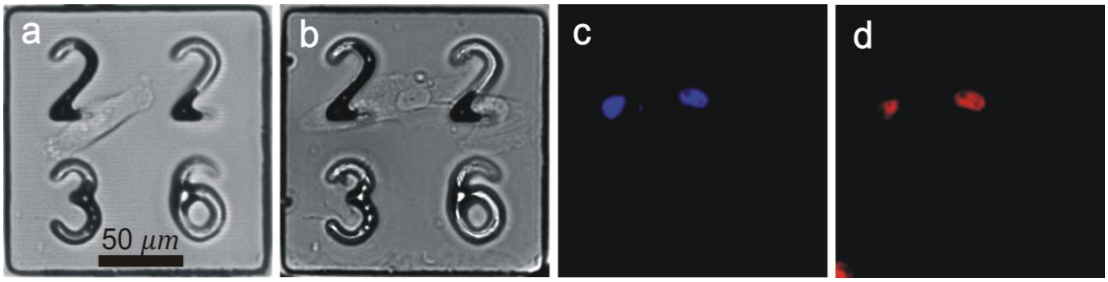

Figure 3.6. Separation of spindle-shaped cells for Pax7 demonstration. a) Brightfield image of spindle-shaped cell growing on 5% AA in PS-coated micropallet before release from array. b) Brightfield image of 5% AA in PS-coated micropallet with cells 48 hrs after release from array. c) Epifluorescence image of cell nuclei from (b) stained with Hoechst dye (blue). d) Epifluorescence image of cell nuclei from (b) stained with Pax7 antibody (red).

plasma-treated glass slide, **Figure 3.6A**. After 48 hrs in culture, the presence of cells was determined with the use of brightfield images and Hoechst staining, **Figure 3.6B and C**. The presence of the transcription factor Pax7 was examined using immunochemistry, **Figure 3.6D**. From this experiment, it was found that 88% of the collected micropallets containing cells possessed Pax7+ cells. Therefore, micropallets containing cells with a spindle-like morphology showed the presence of Pax7 following the separation

procedure, thus demonstrating that PCSCs can be sorted with confidence based on morphology.

Conclusions

A suitable copolymer surface has been developed for the culture of PCSCs atop micropallets. Our results show that the 5% AA-in-PS copolymer mimicked the ability of tissue culture polystyrene in supporting the adhesion and proliferation of the PCSCs. Importantly, cells cultured on this surface showed neither induced differentiation under standard growth conditions nor a rate of spontaneous differentiation greater than that seen with the control TC dish under standard differentiation conditions as indicated by mRNA levels of *Pax7* and *Utrophin*. This copolymer material was readily and consistently applied to the surface of the micropallets using the described contact printing procedure. Experiments using additional contact-printed layers of the ECM proteins collagen and gelatin on the 5% AA-in-PS layer showed no increase in either initial PCSC adhesion or proliferation rates relative to surfaces without the extracellular matrices. The contact-printing method developed in this study is readily applicable to screen thick coatings of almost any polymer matrix for the growth and well-being of primary cells including stem cells. More importantly this should enable, as we have demonstrated, the sorting of primary cells cultured on the arrays based on a number of cellular attributes (morphology and other spatial properties, growth rate and other temporal behaviors) not accessible by current cell separation methods such as preplating and flow cytometry.

Chapter 4

Sorting Primary Canine Satellite Cells with Tri-Partite Micropallet Arrays

Introduction

Muscular dystrophy is a family of diseases that are characterized by progressive dysfunction in the musculature of diseased individuals. Of all the muscular dystrophies, Duchenne muscular dystrophy (DMD) is the most severe form. It affects 1 in 3,500 males and is diagnosed in childhood and leads to muscle degeneration in the teens to early twenties ending in death in the late teens and early twenties. Dystrophin allows cells to transmit forces coming into and leaving muscle cells evenly, lack of dystrophin results in uneven force distribution and damages to cell membranes. By this mechanism, muscles are repeatedly damaged forcing regeneration of the tissue. Repetitive rounds of damage, necrosis and regeneration lead to widespread muscle atrophy, with fibrosis and fatty change as the disease progresses, associated loss of strength and muscle mass.

Cellular therapies to treat DMD are aimed at restoring the strength and mass of the skeletal muscle. Since the host's own cells are diseased, cell therapies require donated cells, allogenic therapy, or correction of the host cells followed by re-implantation, autologous therapy. Both pathways require a population of cells that can support regeneration of the skeletal muscles for the lifetime of the patient. Adult stem cells, found in most if not all tissues are the lead candidates as the cell source to develop cellular therapies for DMD.

To test newly developed therapies along with characterizing new and existing stem cell populations, animal models are commonly used. DMD has two models of primary importance. The first is the muscular dystrophy X-linked (mdx) mouse and the

second is Golden Retriever muscular dystrophy (GRMD). The mouse model has been extensively employed to understand the molecular pathways and disease progression in DMD. However, the mouse model is not entirely consistent with the human disease (Kuhana et al.). The GRMD model is more consistent with the human disease and is a more size relevant model than MDX. For this reason, we are using cells derived from the GRMD model.

Satellite cells are the stem cell of skeletal muscle and as such are responsible for the regenerative capacity of muscle. They are found on the surface of myofibers in a quiescent state until the fiber is damaged, at which time the satellite cell will become activated. Activated cells proliferate and repair damage. Once the damage is fixed some of the proliferating cells can again become quiescent satellite cells.

Pax7 is a transcription factor that is responsible for maintaining quiescent satellite cell populations and allows these cells to again become quiescent. It is considered to be the strongest and most reliable marker of adult satellite cells. Pax7 also inhibits the differentiation of satellite cells and myoblasts. Once myoblasts have up-regulated another transcription factor, myogenin, Pax7 levels fall, allowing the fusion and terminal differentiation of the myoblasts to myotubes. These transcription factors can be used to determine the stem cell state of a given satellite cell.

Stem cells are often characterized by flow cytometry for markers which act as surrogates for stem cell properties. Stem cells have many other properties beyond surface markers that characterize their behavior, characteristics that can't be used to sort cells with a flow cytometer. Additionally, newly discovered stem cells or animal models in the early stages of being characterized may not have the antibody repertoire needed to

fully characterize them, as is the case for GRMD model. Other technologies are needed to sort stem cells based on these alternative properties, including but not limited to proliferation rate, cell morphology, enzymatic function and mobility. One technology that can characterize cells based on these alternative factors and simultaneously be used to sort cells is micropallet array technology [60-63, 112].

Micropallet arrays allow adherent cells to be cultured on a solid surface, which can be modified and adapted to a specific cell type, see **Chapter 3**. Cells can be cultured in clonal fashion on micropallet arrays, important in deciphering stem cell characteristics by eliminating the heterogeneity of multicellular cultures. Micropallets are made using a photolithography technique to cure a photoresist polymer on standard microscope slides [60, 63, 112, 113]. Almost any array pattern can be established to achieve a desired culture scheme. The arrays are then treated with a hydrophobic silane which enables the formation of virtual air walls between the individual pallets [113]. This forces cells to land on the pallet tops and not in between neighboring pallets, **Figure 1.1B**. The top surface of the micropallets can be treated with a number of polymers and proteins to allow for cellular attachment. Once cultures are established, individual pallets can be released with a laser pulse allowing the cells attached to a pallet to be isolated in a less traumatic fashion than trypsinization [63, 112]. Released pallets can then be collected for analysis or placed in a larger culture environment to expand a clonal colony.

Culture and isolation of cells on micropallet arrays has several advantages over flow cytometry. Flow cytometry requires cells to be non-adherent to pass through the machine requiring the use of trypsin or other means of enzymatic digestion to remove the cells from a culture surface. The cells must then be kept on ice and passed through the

flow cytometry apparatus. Cells can be sorted based on many parameters but not for Pax7 expression as it is not a surface protein [74, 97]. Cells can be individually sorted into multiwell plates for clonal expansion. This would then require another trypsinization step in order to obtain some cells for staining with a Pax7 antibody to determine colonies of interest. Micropallet arrays require fewer and less traumatic steps in order to obtain the desired information.

Given the versatility of micropallet array technology and its ability to culture single adherent cells on a culture surface, it can be used to better characterize the stem cell populations derived from muscle. In order to do this, a cell culture format that can allow the clonal culture of cells as well as allow the separation of a given colony into two or more sister colonies is needed. Splitting a clonal colony into multiple sister colonies allows cells to be analyzed for different parameters, including assays that may be destructive to one of the sister colonies. A format of micropallet array, called tri-partite arrays, has been developed to split a clonal colony into two parts, **Figure 4.1**. Cells are seeded onto an array to obtain clonal colonies. Cells that successfully attach to one of the sister pallets can expand numbers and migrate across the bridge pallet to the other sister pallet, effectively splitting the colony into two separable parts.

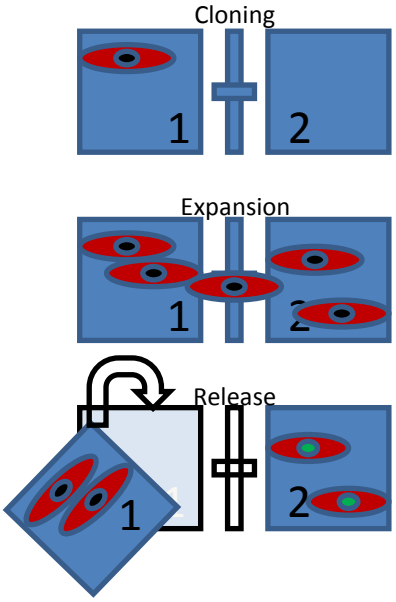

Figure 4.1. Tri-partite pallet culture scheme.

Briefly, satellite cells are seeded onto an array that can contain thousands of individual pallets in a square centimeter which can be covered by a single

milliliter of culture media. This can provide thousands of cloning sites in the small culture area, much more efficient than limiting dilution or flow cytometry cloning of individual cells. Pallets with single adherent cells can be recorded with the aid of an automated microscope and custom software scripts. After an expansion period, the recorded clones are rescanned to determine which colonies expanded and were able to cross the bridge. Half of the bridge pallet containing the clonal cells can then be released, collected for analysis, or cultured. The remaining half of each colony can also be analyzed or further cultured, depending on which format will give the desired information. In the case of satellite cells half of a clonal colony would be released for culture and the remaining half would be stained for Pax7 expression. The cells for culture and eventual transplantation do not have to be exposed to harsh trypsinization nor exposure to antibodies which can alter cell physiology. Utilization of micropallet array technology reduces the amount of stress that cells are put under and reduces the amount of resources, plates, media and time, which are required to obtain the necessary information to identify colonies of interest.

Materials and Methods

Micropallet Array Fabrication and Contact Printing of Polystyrene

Micropallet arrays were fabricated as previously described (see also **Figure 1.1A**) [58, 104]. Briefly, a mask outlining numbered micropallets was used to photolithographically define a 80 × 80 array of 120 × 120 × 50 μm (L x W x H) numbered tripartite micropallets possessing a 60 μm gap between micropallets and a 40 μm gap between sister pallets that contains the bridge element, **Figure 4.2**. Photoresist 1002F was used to

make the pallets. Polyacrylic acid (PAA) (Polysciences Inc., Warrington, PA), 25% in aqueous solution (MW:~50,000) diluted to 8% in DI water, was applied to the upper micropallet surfaces via contact printing [64]. This deposited PAA would serve later as a sacrificial layer to prevent the organosilane ([heptadecafluoro-1,1', 2, 2'-tetrahydrodecyl] trichlorosilane, Gelest, Morrisville, PA) from binding to the top surface of the micropallets. Only arrays possessing ≥90% fully PAA-coated micropallets were used in subsequent steps. Approximately 80% of the arrays met this criterion. The organosilane was applied by vapor-deposition in a vacuum chamber as previously described [58]. Arrays were removed from the chamber, incubated in deionized water for 30 min and rinsed with deionized water to remove the sacrificial PAA layer. Micropallet surfaces were then contact-printed with the polystyrene coating optimized for culture of PCSCs, 5% AA in PS, again only using arrays possessing ≥90% fully polystyrene-coated micropallets in subsequent steps [64]. Again, approximately 80% of the arrays met this criterion. Once printed with polystyrene, arrays were placed in a 60 °C vacuum oven for 48 h to remove any remaining solvent. Arrays were sterilized with 75% ethanol and allowed 30 min to dry. PDMS reservoirs were attached to the slide surface to provide a well for culture media. The PDMS was placed ~2 mm from the edge of the array, on all sides. Uncured liquid PDMS was used to glue the reservoir to the array by placing a small bead of PDMS around the outer perimeter of the reservoir.

Cell Isolations and Culture

PCSCs were isolated from muscle biopsies of the vastus lateralis of a normal dog in the GRMD colony at University of North Carolina at Chapel Hill (UNC-CH). Cells were isolated from biopsies as previously described with minor modifications [65, 81].

Briefly, biopsy material was finely minced and digested with collagenase in growth media, 16.5% FBS in Dulbecco's Modified Eagle Media (DMEM), for 6-8 h. Material was rinsed and digested with 0.05% trypsin for 1 hr with agitation every 15 min. Material was the passed through a 100 μm screen followed by a 40 μm screen and plated on 0.1% gelatin (Millipore, Billerica, MA) coated tissue-culture-treated polystyrene Petri dishes (BD Falcon, Franklin Lakes, NJ). Six successive platings with the preplate procedure resulted in enriched populations of PCSCs, with cells from plates 4, 5, or 6 used in the current experiments [81, 99]. To confirm the presence of PCSCs, 1000 cells from passage two of preplate 5 were fixed and stained with anti-desmin antibodies and counterstained with Hoechst dye. Desmin, a marker for PCSC, was detected in 94% of the cells. The enriched cell populations were further cultured in uncoated TC dishes in 20% fetal bovine serum in Dulbecco's Modified Eagle Medium (DMEM), with 1% penicillin-streptomycin, defined as standard growth conditions [55].

Cells were cultured at a density of 1000 cells per cm^2 and passed every two or three days to prevent overcrowding and spontaneous differentiation. Cultures were not used past passage five to maintain the integrity of the cells. To seed cells on arrays, cells were trypsinized with a trypsin-EDTA solution (SIGMA, St. Louis, MO) for no more than five minutes. Cells were counted with a hemocytometer and diluted down to 3000 cells per mL of growth media. One mL of cell suspension was gently pipetted onto the array to prevent air wall disruption and immediately placed into a tissue culture incubator. After 18 hrs of adhesion, arrays were rinsed with 1 × PBS to remove any non-adherent cells.

Single cell and bridging colony detection

After removal of non-adherent cells, growth media containing 1µg/mL Hoechst dye 33342 was gently pipetted onto the array and allowed to incubate for 10 minutes to permit Hoechst dye to label DNA in cell nuclei. Arrays were then placed on the microscope stage to be scanned. An Olympus IX 81 (Olympus, Center Valley, PA) with an ASI 2000 XY motorized stage was used in conjunction with a custom made Python (Python Software Foundation, Wolfeboro Falls, NH) script to scan the arrays. Individual images are taken of each pallet for brightfield and Hoechst images. A custom Matlab (Mathworks, Natick, MA) script was used to identify pallets with only one nucleus, identified via intensity of Hoechst staining. Arrays were then removed from the microscope and Hoechst containing media was replaced with normal growth media. Cells were allowed to proliferate for an additional 72 hours and then again stained with Hoechst dye to label nuclei, rescanned with the microscope and analyzed for single cell colonies that proliferated and bridged from one sister pallet to the other.

Pax7 and myogenin immunocytochemistry

Following the second scan, arrays were stained with custom labeled antibodies to Pax7 and myogenin transcription factors. Cells on arrays were fixed with a 4% paraformaldehyde solution in 1 × PBS for 10 minutes. Cells were permeabilized with 0.5% Triton X-100 in 1 × PBS for 15 minutes to permit antibody entry into the cell nuclei. Antibodies for Pax7 and myogenin (DSHB, Iowa City, IA) were labeled with an AlexaFluor™ protein labeling kit (Invitrogen, Carlsbad, CA). Pax7 was labeled with Alexa 568 and myogenin with Alexa 488 per manufacturer's instructions. Cells were labeled for 4 hours with a 1:50 dilution of the labeled antibodies in a 1 × PBS solution

containing 2% FBS. Arrays were washed with PBS once for 15 minutes to remove excessive antibodies and covered with 1 × PBS with FBS solution containing 2% FBS. Arrays were then rescanned on the microscope system to image cells.

Results

Arrays with 3200 culture sites were seeded with 3000 cells and scanned at 18 hrs

Figure 4.2. Proliferation of single cell clones and bridge crossing. Single cell colonies identified at 18 hrs after seeding. Proliferation without bridging (A), proliferation with minimal bridging (B), proliferation with robust bridging (C).

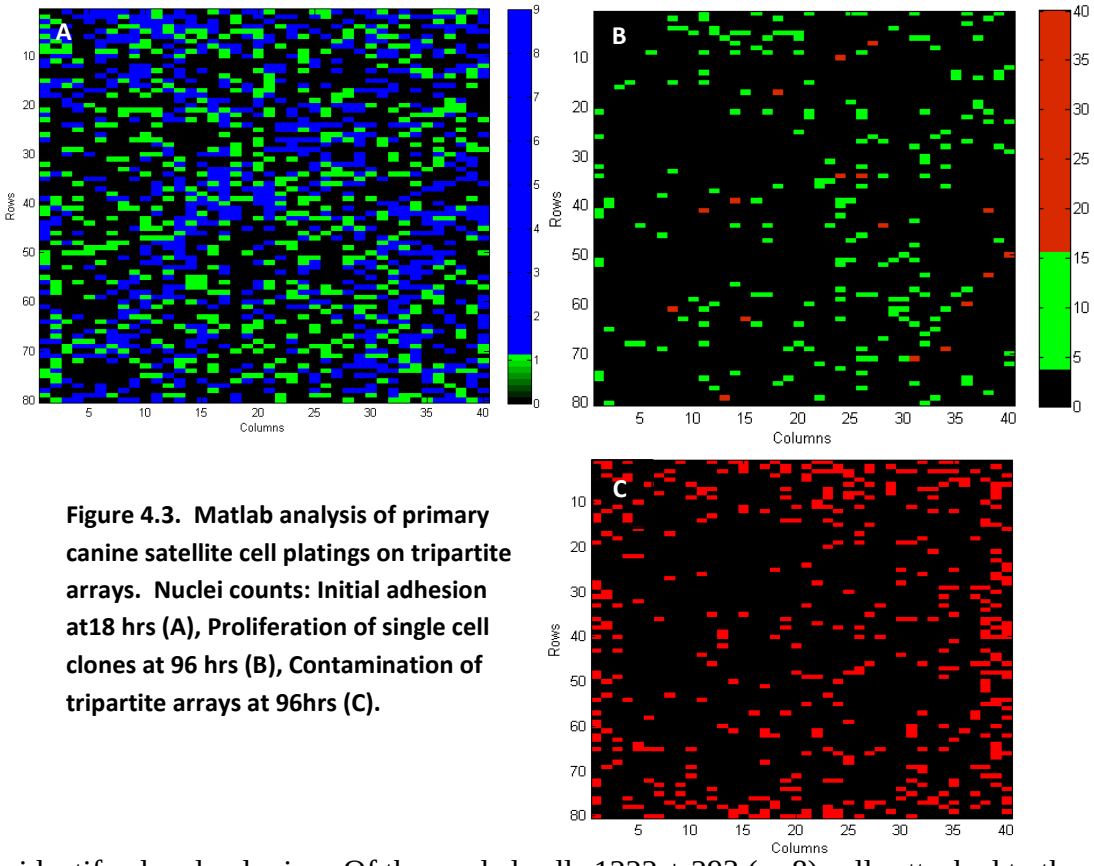

Figure 4.3. Matlab analysis of primary canine satellite cell platings on tripartite arrays. Nuclei counts: Initial adhesion at18 hrs (A), Proliferation of single cell clones at 96 hrs (B), Contamination of tripartite arrays at 96hrs (C).

to identify clonal colonies. Of the seeded cells 1222 ± 293 (n=8) cells attached to the array. Of these 1222 cells, 411 ± 57 (33.6%) were single cell colonies, as determined by

Hoechst staining, **Figure 4.3A**. Cells were allowed to proliferate across the bridging pallet for 72 hours. There were three outcomes for cells: proliferation without bridging, proliferation with minimal bridging, and proliferation with successful bridging, **Figure 4.2 A, B & C** respectively.

General proliferation was considered to be the ability to undergo one or more cell divisions and 166 ± 12 clones (40%) were able to do this, **Figure 4.3 B** (green). 39 ± 9 clones (11%) were able to proliferate with three or more cell divisions, **Figure 4.3 B**

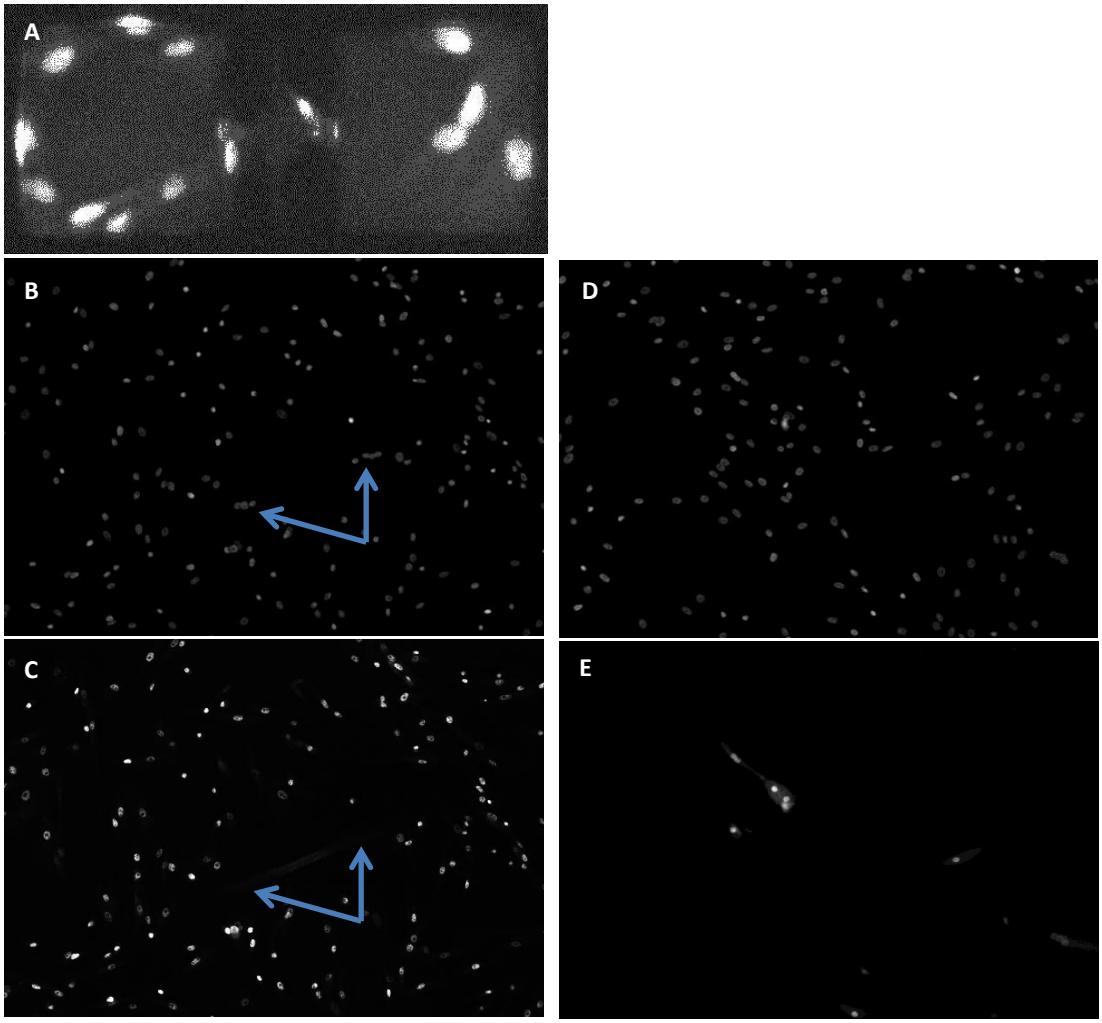

Figure 4.4. Pax7 and Myogenin expression in canine satellite cells. Pax7 expression in a colony of cloned cells at 90 hrs after seeding (left) Hoechst labeled nuclei overlayed on brightfield image (right). (A). Hoechst (B and D), Pax7 (C), and Myogenin (E) staining of canine satellite cell cultures differentiated for 5 days. Arrows indicate nuclei in myotubes in Pax7 (C) and Myogenin (E) cultures.

(red). Contamination was an issue with arrays after 90 hours. All sites without any cells at 18 hrs were identified in the scan. After cells divided for an additional 72 hours and the array rescanned, sites that were previously empty but now contained cells were identified, **Figure 4.3 C** (red). Most of the contamination was around the perimeter of the array.

Arrays were fixed and stained with the pre-labeled antibodies against Pax7 and myogenin. Pax7 was able to successfully label 92% of the nuclei on the array after expansion, at 90 hrs of culture. The original pre-plate isolation for these normal cells, "Pedro" in **Table 2.2**, showed 93% of cells were positive for Pax7, **Figure 4.4C**. Only a few cells stained positive for myogenin protein on any given array.

Discussion

Tri-partite micropallet arrays are a flexible tool that can be used to clone and characterize stem cell populations. The overall size of the array can be modified to obtain the desired number of cloning sites that are needed for analysis. The size of the arrays is also adjustable to any needed configuration. Square pallets with a single crossing point were chosen to streamline the use of scanning software with the tripartite arrays. This may not be the ideal geometry configuration to maximize cloning of satellite cell. A half-moon on each side of the bridge may reduce the amount of distance that a cell has to randomly walk in order to cross the bridge and create a sister colony. Also the size of the arrays could be reduced to further reduce the distance that cells need to migrate and may reduce the time cells need to cross the bridge.

The period of 90 hours was chosen because canine satellite cells divide once every 24 to 36 hrs. This allows cells to divide between three and four times and should allow a clonal colony to reach 8 (2^3) to 16 (2^4) cells per colony. Colonies with fewer than eight cells may not be crowded enough to fully encourage cells to cross over the bridge to the open space of the sister pallet. However, colonies with more than 16 cells at 90 hrs, may have been contaminated with other cells after the first scan at 18 hrs. More information is needed as to the range of proliferative capacity and migratory capabilities of canine satellite cells on micropallets to determine if these colonies can be successfully cloned.

Contamination issues are of concern because this is a continuous media environment that can permit cells that become detached during media changes or moving them back and forth between the microscope and the incubator can compromise the validity of the clonal colonies. There were several "clonal" colonies that had more than 16 cells in the colony, **Figure 4.3B** (red). These could be hyper proliferating stem cells that may be of great interest and value to the muscular dystrophy community or they might just be contaminated cultures that are not valid. Also, there is a large amount of contamination around the periphery of the array. These also happen to be the areas on an array that are most susceptible to air wall breakdown [113]. Some areas lost air wall integrity at the time of seeding allowing cells to fall in between pallets. Canine satellite cells can grow very well on glass slides and can easily contaminate any neighboring pallets. Other areas can suffer air wall breakdown after several hours in the high humidity environment of the cell culture environment. Using larger micropallet arrays may be able to decrease some of the air wall issues leaving more sites open to cloning.

The density of cells may also be reduced to increase the likelihood that a clonal colony is formed and fewer cells on the same number of cloning sites would mean that cells have to travel further to contaminate neighboring pallets that have clonal colonies growing on them.

Tri-partite micropallet arrays can be used to clone primary canine satellite cells and can do so without the loss of Pax7 or induction of myogenin transcription factor expression. Further work needs to be done to characterize cell motility, proliferative capacity and contamination mechanics on the tripartite arrays, in order to validate this as a truly useful single cell cloning and sorting technology.

References

1. Hoffman, E.P., R.H. Brown, Jr., and L.M. Kunkel, *Dystrophin: the protein product of the Duchenne muscular dystrophy locus.* Cell, 1987. **51**(6): p. 919-28.

2. Partridge, T., *The current status of myoblast transfer.* Neurol Sci, 2000. **21**(5 Suppl): p. S939-42.

3. Partridge, T., *Myoblast transplantation.* Neuromuscul Disord, 2002. **12 Suppl 1**: p. S3-6.

4. Quattrocelli, M., et al., *Cell therapy strategies and improvements for muscular dystrophy.* Cell Death Differ, 2010. **17**(8): p. 1222-9.

5. Rando, T.A., G.K. Pavlath, and H.M. Blau, *The fate of myoblasts following transplantation into mature muscle.* Exp Cell Res, 1995. **220**(2): p. 383-9.

6. Wells, D.J. and K.E. Wells, *What do animal models have to tell us regarding Duchenne muscular dystrophy?* Acta Myol, 2005. **24**(3): p. 172-80.

7. Vainzof, M., et al., *Animal models for genetic neuromuscular diseases.* J Mol Neurosci, 2008. **34**(3): p. 241-8.

8. Kornegay, J.N., et al., *Muscular dystrophy in a litter of golden retriever dogs.* Muscle Nerve, 1988. **11**(10): p. 1056-64.

9. Khurana, T.S. and K.E. Davies, *Pharmacological strategies for muscular dystrophy.* Nat Rev Drug Discov, 2003. **2**(5): p. 379-90.

10. DiPrimio, N., S.W. McPhee, and R.J. Samulski, *Adeno-associated virus for the treatment of muscle diseases: toward clinical trials.* Curr Opin Mol Ther, 2010. **12**(5): p. 553-60.

11. Guglieri, M. and K. Bushby, *Molecular treatments in Duchenne muscular dystrophy.* Curr Opin Pharmacol, 2010. **10**(3): p. 331-7.

12. Miyagoe-Suzuki, Y. and S. Takeda, *Gene therapy for muscle disease.* Exp Cell Res, 2010. **316**(18): p. 3087-92.

13. Nishio, H., et al., *Identification of a novel first exon in the human dystrophin gene and of a new promoter located more than 500 kb upstream of the nearest known promoter.* J Clin Invest, 1994. **94**(3): p. 1037-42.

14. Cowan, J., et al., *Incidence of Duchenne muscular dystrophy in New South Wales and Australian Capital Territory.* J Med Genet, 1980. **17**(4): p. 245-9.

15. Caskey, C.T., et al., *Sporadic occurrence of Duchenne muscular dystrophy: evidence for new mutation.* Clin Genet, 1980. **18**(5): p. 329-41.

16. Rapaport, D., et al., *Characterization and cell type distribution of a novel, major transcript of the Duchenne muscular dystrophy gene.* Differentiation, 1992. **49**(3): p. 187-93.

17. Chelly, J., et al., *Transcription of the dystrophin gene in human muscle and non-muscle tissue.* Nature, 1988. **333**(6176): p. 858-60.

18. Blake, D.J., et al., *Function and genetics of dystrophin and dystrophin-related proteins in muscle.* Physiol Rev, 2002. **82**(2): p. 291-329.

19. Dowling, P., P. Doran, and K. Ohlendieck, *Drastic reduction of sarcalumenin in Dp427 (dystrophin of 427 kDa)-deficient fibres indicates that abnormal calcium handling plays a key role in muscular dystrophy.* Biochem J, 2004. **379**(Pt 2): p. 479-88.

20. Khurana, T.S., et al., *Immunolocalization and developmental expression of dystrophin related protein in skeletal muscle.* Neuromuscul Disord, 1991. **1**(3): p. 185-94.

21. Miura, H.S., K. Nakagaki, and F. Taguchi, *N-terminal domain of the murine coronavirus receptor CEACAM1 is responsible for fusogenic activation and conformational changes of the spike protein.* J Virol, 2004. **78**(1): p. 216-23.

22. Rafael, J.A. and S.C. Brown, *Dystrophin and utrophin: genetic analyses of their role in skeletal muscle.* Microsc Res Tech, 2000. **48**(3-4): p. 155-66.

23. Dubowitz, V., *Muscle Disorders in Childhoold*. 2nd ed. 1995, Philadelphia, PA: W.B. Saunders Co.

24. Emery, A.M., F., *Duchenne Muscular Dystrophy*. 2003: Oxford University Press.

25. Sharp, N.J.H., et al., *Notexin-Induced Muscle Injury in the Dog.* Journal of the Neurological Sciences, 1993. **116**(1): p. 73-81.

26. Schatzberg, S.J., et al., *Alternative dystrophin gene transcripts in golden retriever muscular dystrophy.* Muscle Nerve, 1998. **21**(8): p. 991-8.

27. Schatzberg, S.J., et al., *Molecular analysis of a spontaneous dystrophin 'knockout' dog.* Neuromuscul Disord, 1999. **9**(5): p. 289-95.

28. Angelini, C., *The role of corticosteroids in muscular dystrophy: a critical appraisal.* Muscle Nerve, 2007. **36**(4): p. 424-35.

29. Liu, J.M., et al., *Effects of prednisone in canine muscular dystrophy.* Muscle Nerve, 2004. **30**(6): p. 767-73.

30. Pichavant, C., et al., *Current status of pharmaceutical and genetic therapeutic approaches to treat DMD.* Mol Ther, 2011. **19**(5): p. 830-40.

31. Olsen, J.C., *EIAV, CAEV and other lentivirus vector systems.* Somat Cell Mol Genet, 2001. **26**(1-6): p. 131-45.
32. Wang, B., J. Li, and X. Xiao, *Adeno-associated virus vector carrying human minidystrophin genes effectively ameliorates muscular dystrophy in mdx mouse model.* Proc Natl Acad Sci U S A, 2000. **97**(25): p. 13714-9.
33. Wang, B., et al., *A canine minidystrophin is functional and therapeutic in mdx mice.* Gene Ther, 2008. **15**(15): p. 1099-106.
34. Collins, C.A., et al., *Stem cell function, self-renewal, and behavioral heterogeneity of cells from the adult muscle satellite cell niche.* Cell, 2005. **122**(2): p. 289-301.
35. Partridge, T.A., M. Grounds, and J.C. Sloper, *Evidence of fusion between host and donor myoblasts in skeletal muscle grafts.* Nature, 1978. **273**(5660): p. 306-8.
36. Partridge, T.A., et al., *Conversion of mdx myofibres from dystrophin-negative to -positive by injection of normal myoblasts.* Nature, 1989. **337**(6203): p. 176-9.
37. Watt, D.J., J.E. Morgan, and T.A. Partridge, *Use of mononuclear precursor cells to insert allogeneic genes into growing mouse muscles.* Muscle Nerve, 1984. **7**(9): p. 741-50.
38. Gussoni, E., et al., *Normal dystrophin transcripts detected in Duchenne muscular dystrophy patients after myoblast transplantation.* Nature, 1992. **356**(6368): p. 435-8.
39. Gussoni, E., H.M. Blau, and L.M. Kunkel, *The fate of individual myoblasts after transplantation into muscles of DMD patients.* Nat Med, 1997. **3**(9): p. 970-7.
40. Law, P.K., et al., *First human myoblast transfer therapy continues to show dystrophin after 6 years.* Cell Transplant, 1997. **6**(1): p. 95-100.
41. Arsic, N., et al., *Muscle-derived stem cells isolated as non-adherent population give rise to cardiac, skeletal muscle and neural lineages.* Exp Cell Res, 2008. **314**(6): p. 1266-80.
42. Arthur, A., A. Zannettino, and S. Gronthos, *The therapeutic applications of multipotential mesenchymal/stromal stem cells in skeletal tissue repair.* J Cell Physiol, 2009. **218**(2): p. 237-45.
43. Asakura, A. and M.A. Rudnicki, *Side population cells from diverse adult tissues are capable of in vitro hematopoietic differentiation.* Exp Hematol, 2002. **30**(11): p. 1339-45.
44. Cao, B., et al., *Muscle stem cells differentiate into haematopoietic lineages but retain myogenic potential.* Nat Cell Biol, 2003. **5**(7): p. 640-6.
45. Dezawa, M., et al., *Bone marrow stromal cells generate muscle cells and repair muscle degeneration.* Science, 2005. **309**(5732): p. 314-7.
46. Shi, D., et al., *Myogenic fusion of human bone marrow stromal cells, but not hematopoietic cells.* Blood, 2004. **104**(1): p. 290-4.

47. Dell'Agnola, C., et al., *Hematopoietic stem cell transplantation does not restore dystrophin expression in Duchenne muscular dystrophy dogs.* Blood, 2004. **104**(13): p. 4311-8.

48. Bretag, A.H., *Stem cell treatment of dystrophic dogs.* Nature, 2007. **450**(7173): p. E23; discussion E23-5.

49. Cossu, G., et al., *Activation of different myogenic pathways: myf-5 is induced by the neural tube and MyoD by the dorsal ectoderm in mouse paraxial mesoderm.* Development, 1996. **122**(2): p. 429-37.

50. De Angelis, L., et al., *Skeletal myogenic progenitors originating from embryonic dorsal aorta coexpress endothelial and myogenic markers and contribute to postnatal muscle growth and regeneration.* J Cell Biol, 1999. **147**(4): p. 869-78.

51. Minasi, M.G., et al., *The meso-angioblast: a multipotent, self-renewing cell that originates from the dorsal aorta and differentiates into most mesodermal tissues.* Development, 2002. **129**(11): p. 2773-83.

52. Sampaolesi, M., et al., *Mesoangioblast stem cells ameliorate muscle function in dystrophic dogs.* Nature, 2006. **444**(7119): p. 574-9.

53. Galvez, B.G., et al., *Complete repair of dystrophic skeletal muscle by mesoangioblasts with enhanced migration ability.* J Cell Biol, 2006. **174**(2): p. 231-43.

54. Buckingham, M., et al., *The formation of skeletal muscle: from somite to limb.* J Anat, 2003. **202**(1): p. 59-68.

55. Burton, N.M., et al., *Methods for animal satellite cell culture under a variety of conditions.* Methods Cell Sci, 2000. **22**(1): p. 51-61.

56. Kuang, S., et al., *Asymmetric self-renewal and commitment of satellite stem cells in muscle.* Cell, 2007. **129**(5): p. 999-1010.

57. Michal, J., et al., *Isolation and characterization of canine satellite cells.* In Vitro Cell Dev Biol Anim, 2002. **38**(8): p. 467-80.

58. Salazar, G.T., et al., *Micropallet arrays for the separation of single, adherent cells.* Anal Chem, 2007. **79**(2): p. 682-7.

59. Sims, C.E., et al., *Choosing one from the many: selection and sorting strategies for single adherent cells.* Anal Bioanal Chem, 2007. **387**(1): p. 5-8.

60. Wang, Y., et al., *Broadening cell selection criteria with micropallet arrays of adherent cells.* Cytometry A, 2007. **71**(10): p. 866-74.

61. Quinto-Su, P.A., et al., *Mechanisms of pulsed laser microbeam release of SU-8 polymer "micropallets" for the collection and separation of adherent cells.* Anal Chem, 2008. **80**(12): p. 4675-9.

62. Shadpour, H., C.E. Sims, and N.L. Allbritton, *Enrichment and expansion of cells using antibody-coated micropallet arrays.* Cytometry A, 2009. **75**(7): p. 609-18.

63. Wang, Y., et al., *Collection and expansion of single cells and colonies released from a micropallet array.* Anal Chem, 2007. **79**(6): p. 2359-66.

64. Xu, W., et al., *Contact printing of arrayed microstructures.* Anal Bioanal Chem, 2010. **397**(8): p. 3377-85.

65. Jankowski, R.J., B.M. Deasy, and J. Huard, *Muscle-derived stem cells.* Gene Ther, 2002. **9**(10): p. 642-7.

66. Kang, J.S. and R.S. Krauss, *Muscle stem cells in developmental and regenerative myogenesis.* Curr Opin Clin Nutr Metab Care, 2010. **13**(3): p. 243-8.

67. Schultz, E. and K.M. McCormick, *Skeletal muscle satellite cells.* Rev Physiol Biochem Pharmacol, 1994. **123**: p. 213-57.

68. Kornegay, J.N., et al., *Canine models of Duchenne muscular dystrophy and their use in therapeutic strategies.* Mamm Genome, 2012. **23**(1-2): p. 85-108.

69. Mauro, A., *Satellite cell of skeletal muscle fibers.* J Biophys Biochem Cytol, 1961. **9**: p. 493-5.

70. Armand, O., et al., *Origin of satellite cells in avian skeletal muscles.* Arch Anat Microsc Morphol Exp, 1983. **72**(2): p. 163-81.

71. Ben-Yair, R., N. Kahane, and C. Kalcheim, *Coherent development of dermomyotome and dermis from the entire mediolateral extent of the dorsal somite.* Development, 2003. **130**(18): p. 4325-36.

72. Schienda, J., et al., *Somitic origin of limb muscle satellite and side population cells.* Proc Natl Acad Sci U S A, 2006. **103**(4): p. 945-50.

73. Halevy, O., et al., *Pattern of Pax7 expression during myogenesis in the posthatch chicken establishes a model for satellite cell differentiation and renewal.* Dev Dyn, 2004. **231**(3): p. 489-502.

74. Seale, P., et al., *Pax7 is required for the specification of myogenic satellite cells.* Cell, 2000. **102**(6): p. 777-86.

75. Kuang, S., et al., *Distinct roles for Pax7 and Pax3 in adult regenerative myogenesis.* J Cell Biol, 2006. **172**(1): p. 103-13.

76. Day, K., B. Paterson, and Z. Yablonka-Reuveni, *A distinct profile of myogenic regulatory factor detection within Pax7+ cells at S phase supports a unique role of Myf5 during posthatch chicken myogenesis.* Dev Dyn, 2009. **238**(4): p. 1001-9.

77. Sabourin, L.A. and M.A. Rudnicki, *The molecular regulation of myogenesis.* Clin Genet, 2000. **57**(1): p. 16-25.

78. Figarella-Branger, D., et al., *Sequence of expression of MyoD1 and various cell surface and cytoskeletal proteins in regenerating mouse muscle fibers following treatment with sodium dihydrogen phosphate.* J Neurol Sci, 1999. **170**(2): p. 151-60.

79. Gramolini, A.O. and B.J. Jasmin, *Expression of the utrophin gene during myogenic differentiation.* Nucleic Acids Res, 1999. **27**(17): p. 3603-9.

80. Jankowski, R.J. and J. Huard, *Establishing reliable criteria for isolating myogenic cell fractions with stem cell properties and enhanced regenerative capacity.* Blood Cells Mol Dis, 2004. **32**(1): p. 24-33.

81. Rando, T.A. and H.M. Blau, *Primary mouse myoblast purification, characterization, and transplantation for cell-mediated gene therapy.* J Cell Biol, 1994. **125**(6): p. 1275-87.

82. Conboy, I.M., *Protocols for adult stem cells [electronic resource]*. Methods in molecular biology, 1064-3745 ; 621Springer protocols, ed. I.M. Conboy. 2010, New York: Humana.

83. Jankowski, R.J., et al., *Flow cytometric characterization of myogenic cell populations obtained via the preplate technique: potential for rapid isolation of muscle-derived stem cells.* Hum Gene Ther, 2001. **12**(6): p. 619-28.

84. Nakagaki, K.e.a., *A quantitative comparison of NCAM-positive muscle cells from normal and dystrophic dogs.* Muscle Nerve, 1994. **17**(Supplement 1): p. S193.

85. Prattis, S.M., et al., *Magnetic affinity cell sorting (MACS) separation and flow cytometric characterization of neural cell adhesion molecule-positive, cultured myogenic cells from normal and dystrophic dogs.* Exp Cell Res, 1993. **208**(2): p. 453-64.

86. Berg, Z., et al., *Muscle satellite cells from GRMD dystrophic dogs are not phenotypically distinguishable from wild type satellite cells in ex vivo culture.* Neuromuscul Disord, 2011. **21**(4): p. 282-90.

87. Blau, H.M., C. Webster, and G.K. Pavlath, *Defective myoblasts identified in Duchenne muscular dystrophy.* Proc Natl Acad Sci U S A, 1983. **80**(15): p. 4856-60.

88. Cossu, G., et al., *In vitro differentiation of satellite cells isolated from normal and dystrophic mammalian muscles. A comparison with embryonic myogenic cells.* Cell Differ, 1980. **9**(6): p. 357-68.

89. Dubois, C., et al., *Expression of NCAM and its polysialylated isoforms during mdx mouse muscle regeneration and in vitro myogenesis.* Neuromuscul Disord, 1994. **4**(3): p. 171-82.

90. Melone, M.A., et al., *Defective growth in vitro of Duchenne Muscular Dystrophy myoblasts: the molecular and biochemical basis.* J Cell Biochem, 1999. **76**(1): p. 118-32.

91. Valentine, B.A., et al., *In vitro characteristics of normal and dystrophic skeletal muscle from dogs.* Am J Vet Res, 1991. **52**(1): p. 104-7.

92. Yablonka-Reuveni, Z. and J.E. Anderson, *Satellite cells from dystrophic (mdx) mice display accelerated differentiation in primary cultures and in isolated myofibers.* Dev Dyn, 2006. **235**(1): p. 203-12.

93. Ellmers, L.J., et al., *Ventricular expression of natriuretic peptides in Npr1(-/-) mice with cardiac hypertrophy and fibrosis.* Am J Physiol Heart Circ Physiol, 2002. **283**(2): p. H707-14.

94. Livak, K.J. and T.D. Schmittgen, *Analysis of relative gene expression data using real-time quantitative PCR and the 2(T)(-Delta Delta C) method.* Methods, 2001. **25**(4): p. 402-408.

95. Schefe, J.H., et al., *Quantitative real-time RT-PCR data analysis: current concepts and the novel "gene expression's C(T) difference" formula.* Journal of Molecular Medicine-Jmm, 2006. **84**(11): p. 901-910.

96. Charge, S.B. and M.A. Rudnicki, *Cellular and molecular regulation of muscle regeneration.* Physiol Rev, 2004. **84**(1): p. 209-38.

97. Olguin, H.C. and B.B. Olwin, *Pax-7 up-regulation inhibits myogenesis and cell cycle progression in satellite cells: a potential mechanism for self-renewal.* Dev Biol, 2004. **275**(2): p. 375-88.

98. Barjot, C., et al., *Expression of myosin heavy chain and of myogenic regulatory factor genes in fast or slow rabbit muscle satellite cell cultures.* J Muscle Res Cell Motil, 1995. **16**(6): p. 619-28.

99. Jankowski, R.J. and J. Huard, *Myogenic cellular transplantation and regeneration: sorting through progenitor heterogeneity.* Panminerva Med, 2004. **46**(1): p. 81-91.

100. Qu, Z., et al., *Development of approaches to improve cell survival in myoblast transfer therapy.* J Cell Biol, 1998. **142**(5): p. 1257-67.

101. Webster, C., et al., *The myoblast defect identified in Duchenne muscular dystrophy is not a primary expression of the DMD mutation. Clonal analysis of myoblasts from five double heterozygotes for two X-linked loci: DMD and G6PD.* Hum Genet, 1986. **74**(1): p. 74-80.

102. Sacco, A., et al., *Short telomeres and stem cell exhaustion model Duchenne muscular dystrophy in mdx/mTR mice.* Cell, 2010. **143**(7): p. 1059-71.

103. Gunn, N.M., et al., *Fabrication and biological evaluation of uniform extracellular matrix coatings on discontinuous photolithography generated micropallet arrays.* J Biomed Mater Res A, 2010. **95**(2): p. 401-12.

104. Pai, J.H., et al., *Photoresist with low fluorescence for bioanalytical applications.* Anal Chem, 2007. **79**(22): p. 8774-80.

105. Beaulieu, I., M. Geissler, and J. Mauzeroll, *Oxygen plasma treatment of polystyrene and Zeonor: substrates for adhesion of patterned cells.* Langmuir, 2009. **25**(12): p. 7169-76.

106. Dhayal, M., M.R. Alexander, and J.W. Bradley, *The surface chemistry resulting from low-pressure plasma treatment of polystyrene: The effect of residual vessel bound oxygen.* Applied Surface Science, 2006. **252**(22): p. 7957-7963.

107. Coopman, P.J., et al., *Phagocytosis of cross-linked gelatin matrix by human breast carcinoma cells correlates with their invasive capacity.* Clin Cancer Res, 1998. **4**(2): p. 507-15.

108. Gardel, M. and U. Schwarz, *Cell-substrate interactions.* J Phys Condens Matter, 2010. **22**(19): p. 190301.

109. Levy-Mishali, M., J. Zoldan, and S. Levenberg, *Effect of scaffold stiffness on myoblast differentiation.* Tissue Eng Part A, 2009. **15**(4): p. 935-44.

110. Lee, J.H., et al., *Cell behaviour on polymer surfaces with different functional groups.* Biomaterials, 1994. **15**(9): p. 705-11.

111. Deasy, B.M., R.J. Jankowski, and J. Huard, *Muscle-derived stem cells: characterization and potential for cell-mediated therapy.* Blood Cells Mol Dis, 2001. **27**(5): p. 924-33.

112. Salazar, G.T., et al., *Characterization of the laser-based release of micropallets from arrays.* J Biomed Opt, 2008. **13**(3): p. 034007.

113. Wang, Y., et al., *Stability of virtual air walls on micropallet arrays.* Anal Chem, 2007. **79**(18): p. 7104-9.